

AD-A052 915

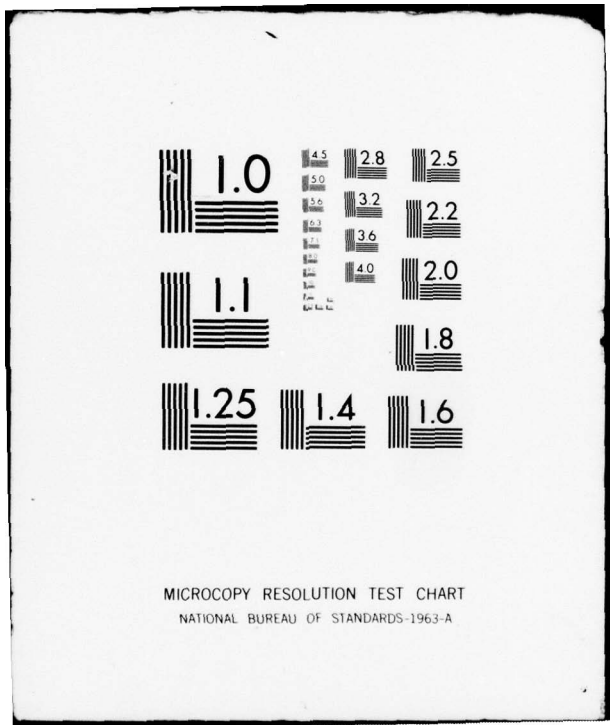
AIR FORCE INST OF TECH WRIGHT-PATTERSON AFB OHIO SCH--ETC F/G 20/5
PHASE-LOCK CONTROL CONSIDERATIONS FOR MULTIPLE, COHERENTLY COMB--ETC(U)
DEC 77 J B ARMOR

UNCLASSIFIED

AFIT/6E0/EE/77-2

NL

1 OF 2
AD
A052915



MICROCOPY RESOLUTION TEST CHART
NATIONAL BUREAU OF STANDARDS-1963-A

AD A 052915

No. _____
ODC FILE COPY



UNITED STATES AIR FORCE
 AIR UNIVERSITY
 AIR FORCE INSTITUTE OF TECHNOLOGY
 Wright-Patterson Air Force Base, Ohio

DDC
 RECEIVED
 APR 20 1978
 A

DISTRIBUTION STATEMENT A
 Approved for public release
 Distribution Unlimited

1
①

AD NO. /
DDC FILE COPY

AD A 052915

PHASE-LOCK CONTROL CONSIDERATIONS
FOR MULTIPLE, COHERENTLY
COMBINED LASERS

THESIS

AFIT/GEO/EE/77-2 James B. Armor, Jr.
Captain USAF

DDC
RECEIVED
APR 20 1978
A

AFIT/GE0/EE/77-2

14

6

PHASE-LOCK CONTROL CONSIDERATIONS
FOR MULTIPLE, COHERENTLY
COMBINED LASERS.

9

Master's THESIS,

Presented to the Faculty of the School of Engineering
of the Air Force Institute of Technology
Air University
in Partial Fulfillment of the
Requirements for the Degree of
Master of Science

10

by
~~STON~~
James B. Armor, Jr

Captain USAF

Graduate Electro-Optics

11

December 1977

12

123 p.

ACCESSION IN	
NTIS	Write Section <input checked="" type="checkbox"/>
DTIC	Buy Section <input type="checkbox"/>
UNANNOUNCED	<input type="checkbox"/>
JUSTIFICATION	
BY	
DISTRIBUTION AVAILABILITY CODES	
Dist	AVAIL. END. OR SPECIAL
A	

Approved for public release; distribution unlimited

012 225

mt

Preface

This work combines several diverse fields of study to develop a potentially realizable laser phase locked array system. Phaselock techniques, control theory, signal detection, and laser physics were all required to analyze the system's performance. This paper assumes the reader has a working knowledge of random processes and Fourier and Laplace transforms.

I was fortunate to have had as my advisor Captain Stanley R. Robinson whose critical comments and direction I gratefully acknowledge. With his skillful guidance and patient friendship this work changed from just a thesis into a nearly overwhelming personal learning experience not only in textbook knowledge but in self knowledge as well. For this personal growth I am eternally grateful.

I would also like to thank the men of the GEO-77D section, especially Captain R. Stanley Shinkle, Captain Barry W. Lyons, and Captain Hal E. Hagemeyer for their comradeship and exchange of ideas.

Finally, my wife, Mary, deserves much more than a simple thanks for the typing and moral support she has given me throughout this task.

James B. Armor, Jr.

Contents

	Page
Preface	ii
List of Figures	v
List of Tables	vii
Notation	viii
Abstract	xvi
I. Introduction	1
II. Two-Laser Control Loop	4
Basic Phaselock Loop	4
Pairwise Laser Phaselock	8
VCO Output	9
Loop Reference Input	13
Phase Detector Output	13
Loop Filter Output	14
Loop Equation	14
Statistical Description of Loop Noise Sources	18
Loop Reference Instabilities	18
Laser Phase Instabilities	19
Heterodyne Receiver Noise	20
Steady State, Second Moment Description of the Laser Pair Differential Phase	22
Noise Equivalent Bandwidth Model of the Closed-Loop Transfer Function	23
Steady State Mean	25
Steady State Variance	26
Two-Laser Loop Design Considerations	29
Minimum Phase Variance Bandwidth	30
Loop Filter Requirements	32
Loop Dynamic Effects	38
Loop Reference Instability	43
Numerical Design Example	45
III. Laser Arrays	53
Single Reference Array	54
Sequential Array	60
Laser Array Design Considerations	62
Loop Reference Control	63
Single Versus Separate Detectors	63
Stability of the Reference Laser	64

	Page
Initial Acquisition	65
Beam Control	66
IV. Conclusion	68
Summary	68
Suggestions for Further Study	70
Bibliography	73
Appendix A: Heterodyne Detection	75
Appendix B: Laser Phase Instabilities	81
Appendix C: Laser Frequency Modulation	95
Appendix D: Quadrature Component Representation of Narrowband Noise	100

List of Figures

Figure		Page
1	Basic Phaselock Loop	4
2	Equivalent Linear Filter Model of the Phaselock Loop	7
3	Two-Laser Differential Phase Control Loop . . .	9
4	Linear Two-Laser Phaselock Loop Model	16
5	Equivalent Linear Filter Model of the Two-Laser Phaselock Loop for (a) Laplace and (b) Time Domains	17
6	Noise Equivalent Bandwidth Model of the Closed Loop Transfer Function	24
7	Graphical Representation of Contributions to the Laser Differential Phase Error Variance due to (a) the Heterodyne Receiver Noise and (b) the Lasers' Phase Instabilities	27
8	Closed Loop Bandwidth versus Laser Differential Phase Error Variance	31
9	Laser Array Control Loops	55
10	Array Design Tradeoffs in the Frequency Domain (N=6)	59
11	Representation of Beam Sampling Optics for a Sequential Array	60
A-1	Basic Heterodyne Receiver Configuration	75
A-2	Heterodyne Receiver Bandpass Filter Transfer Function	78
A-3	Multiple Heterodyne Receiver Configuration . . .	80
A-4	Multiple Heterodyne Receiver BPF Array Transfer Function. (Each cell need not have the same magnitude.)	80
B-1	Phasor Representation of Laser Instabilities . .	82

Figure	Page
B-2 Typical Arrangement for Measuring the Spectra of a Laser Field and Its Instantaneous Frequency	84
C-1 External Crystal Frequency Modulation Configuration	96
C-2 Internal Crystal Frequency Modulation Configuration	97
D-1 Spectra of (a) Narrowband Noise and (b) Quad- rature Components of the Narrowband Noise with $S_n(f)$ Symmetric about f_d (Ref 22:242)	101

List of Tables

Table		Page
I	Basic Parameters for First, Second and Third Order Loop Filters	33
II	Control Modulation Schemes in Temporal and Laplace Representation	34
III	Mean, Steady State Value of the Laser Differential Phase for Different Loop Orders and Modulation Schemes	37
IV	Equations for Dynamic Performance of a Second-Order Phaselock Loop in the Absence of Noise	40

Notation

a	Loop filter coefficient
A	Amplitude of the laser field (volts/meter $\sqrt{\text{ohm}}$) (subscripted by the number of the laser it represents)
A_d	Active area of the optical detector (meters ²)
b	Loop filter coefficient
$b(t)$	Heterodyne receiver bandpass filter impulse response
$B(j2\pi f)$	Heterodyne receiver bandpass filter transfer function
B_{nm}	Bandwidth of the heterodyne receiver bandpass filter for the control loop pairing the nth and mth laser (Hz)
BPF	Bandpass filter
c_a	Rate of the modulation control signal acceleration (volts/sec ²)
$c_n(t)$	In-phase component of laser field noise $M(t)$ (volts/meters $\sqrt{\text{ohm}}$)
c_r	Slope of the modulation control signal ramp (volts/sec)
c_s	Magnitude of the modulation control signal step (volts)
$1/C_{01}$	Magnitude of the heterodyne receiver bandpass filter
\hat{C}_1	Phase variance equation coefficient due to HR noise (sec)
\hat{C}_2	Phase variance equation coefficient due to quantum laser instabilities (sec ⁻¹)
\hat{C}_3	Phase variance equation coefficient due to external laser instabilities (sec ⁻²)

\hat{C}_{1n}	\hat{C}_1 for the nth control loop
\hat{C}_{2n}	\hat{C}_2 for the nth control loop
\hat{C}_{3n}	\hat{C}_3 for the nth control loop
d	Width of the laser modulation crystal across which the voltage is applied (m)
d_{PE}	Piezoelectric crystal coefficient (meter/volt)
D	Modulated reference phase acceleration rate (frequency ramp) (rad/sec^2)
D_{\max}	Maximum tracking frequency sweep rate (rad/sec^2)
$e_n(t)$	Modulation control signal for the nth control loop (volts)
e_{ldc}	Time constant portion of the modulation control signal for the two-laser control loop (volt)
$e_{lmod}(t)$	Time varying portion of the modulation control signal for the two-laser control loop (volts)
$E[\]$	Ensemble average of the quantity in brackets (expected value)
$E[\]_{ss}$	Steady state, expected value of the quantity in brackets
EO	Electro-optic crystal
$E_n(s)$	Laplace transform of $e_n(t)$
$E(\vec{r}, t)$	Spacial and time dependent laser electric field (subscripted by number of laser it represents)
$E(t)$	Time dependent laser electric field
f	Frequency (Hz)
$f(t)$	Loop filter's impulse response
f_c	Cutoff frequency (Hz)
f_d	Frequency difference between two lasers (Hz)

f_n	Operating frequency of the nth laser (Hz)
f_{nq}	Quiescent frequency of the nth laser (Hz)
Δf	Frequency step in the modulated reference phase (Hz)
Δf_{cav}	Cold cavity, FWHM bandwidth of a laser resonator (Hz)
Δf_e	Laser field spectrum linewidth (FWHM) due to external laser phase noise (Hz)
Δf_q	Laser field spectrum linewidth (FWHM) due to quantum laser phase noise (Hz)
$F(s)$	Loop filter transfer function
FWHM	Full width at half maximum
h	Planck's constant (6.63×10^{-34} joule-sec)
$h(t)$	Closed-loop filter impulse response
$H(s)$	Closed-loop filter transfer function
HR	Heterodyne receiver
Hz	Hertz (cycles/sec)
$i_d(t)$	Heterodyne receiver output current (amps)
K	Loop constant (sec^{-1})
K_d	Phase detector gain (1/volt)
K_m	Laser crystal modulator gain (Hz/volt)
l	Length of the modulator crystal (meters)
Δl	Change in the Piezoelectric crystal length with applied voltage (meters)
L	Length of the laser resonator cavity (meters)
L'	Length of the laser cavity less the length of an internally mounted crystal (meters)
$L_p []$	The lowpass portion of the quantity in brackets

L_λ	Optical length of the laser resonator cavity (meters)
ΔL_λ	Change in the optical length of the laser cavity with voltage applied to a modulator crystal (meters)
$L[]$	The Laplace transform of the quantity in brackets
$L^{-1}[]$	The inverse Laplace transform of the quantity in brackets
m	Laser index number ($m=0,1,2,\dots,N$)
$M(t)$	Random process representing the additive random noise of a laser field (volts/meter $\sqrt{\text{ohm}}$)
n	Laser index number ($n=0,1,2,\dots,N$)
$n_c(t)$	In-phase component of heterodyne receiver noise $n(t)$ (volts)
$n_s(t)$	Quadrature component of heterodyne receiver noise $n(t)$ (volts)
$n(t)$	Random process representing heterodyne receiver noise (volts)
$n'(t)$	Random process representing the loop phase noise due to the heterodyne receiver noise (rad)
n_o	Index of refraction of an electro-optic modulator crystal
Δn_o	Change in the index of refraction of an electro-optic modulator crystal when voltage is applied
N	Number of laser pairs in a laser array (\equiv number of modulated lasers in a laser array)
NEB	Noise equivalent bandwidth
$N'(s)$	Laplace transform of $n'(t)$
N_r	Power spectral density magnitude of the reference phase noise
N_2	Population of the upper laser transition level
ΔN	Population difference between the upper and lower laser transition levels

P	Power out of a laser (watts)
PD	Phase detector
PE	Piezoelectric crystal
q	Charge of an electron (1.60×10^{19} coul)
\bar{r}	Spacial position with respect to arbitrary reference axes (meters)
r_{EO}	Electro-optic crystal coefficient (meters/volt)
R	Resistance (ohms)
$\text{Re} [\]$	The real part of the quantity in brackets
R_{\max}	Maximum acquisition frequency sweep rate (rad/sec ²)
$R(t_2, t_1)$ $=R(t+\tau, t)$	Autocorrelation of a nonstationary process (subscripted by the variable whose autocorrelation it represents)
$R(\tau)$	Autocorrelation of a stationary process (subscripted by the variable whose autocorrelation it represents)
$R(0)$	Variance of a stationary process (subscripted by the variable whose variance it represents)
R_1	Reflectivity of the front laser cavity mirror
R_2	Reflectivity of the rear laser cavity mirror
s	Laplace operator
$s_n(t)$	Quadrature component of the laser field noise $M(t)$ (volt/meter $\sqrt{\text{ohm}}$)
$S(f)$	Power spectral density or "spectrum"
t	Time (sec)
T_L	Lock-in time (sec)
T_P	Pull-in time (sec)
u	Dummy variable used in integrations

$u(t)$	Step function (=1 for $t \geq 0$ and 0 elsewhere)
$v(t)$	Time varying signal (volts)
$v_d(t)$	VCO output signal (i.e., heterodyne receiver output) (volts)
$v_e(t)$	Phase detector output signal (volts)
$v_f(t)$	Loop filter output signal (volts)
$v_r(t)$	Loop reference signal (volts)
VCO	Voltage controlled oscillator
V_d	Amplitude of $v_d(t)$ (volts)
$V_e(s)$	Laplace transform of $v_e(t)$
$V_f(s)$	Laplace transform of $v_f(t)$
V_r	Amplitude of $v_r(t)$ (volts)
W_H	Closed loop transfer function noise equivalent bandwidth (Hz)
W_{Hmin}	Value of W_H for which the laser differential phase variance is minimized
$x(t)$	Defined as $\exp j\gamma(t)$
$y(t)$	Defined as $\delta(t+\tau) - \delta(t)$
$Y(f)$	Fourier transform of $y(t)$
α_n	Defined as $\Delta f_q / 2\pi$ for the nth laser (Hz)
α_l	Average distributed field loss per pass in a laser cavity (cm^{-1})
β_n	Defined as $\Delta f_e^2 / 8\pi \ln 2$ for the nth laser (Hz^2)
$\gamma(t)$	Random process representing phase instabilities
$\gamma_d(t)$	Differential phase instabilities of the locked laser pair
$\gamma_e(t)$	Differential phase instabilities of the locked laser pair due to external laser noise

$\gamma_q(t)$	Differential phase instabilities of the locked laser pair due to laser quantum noise
$\gamma_r(t)$	Phase instabilities of the reference signal
$\Delta\gamma(t, \tau)$	Defined as $\gamma(t+\tau) - \gamma(t)$
$\Gamma_d(s)$	Laplace transform of $\gamma_d(t)$
$\Gamma_r(s)$	Laplace transform of $\gamma_r(t)$
$\delta(t)$	Dirac delta (=1 for $t=0$, and 0 elsewhere)
$\zeta(t)$	Reference phase control modulation (rad)
$Z(s)$	Laplace transform of $\gamma(t)$
η	Quantum efficiency of an optical detector (photo-electrons/photon)
$\theta_d(t)$	Modulated portion of the laser differential phase (rad)
$\theta_r(t)$	Modulated portion of the reference phase (rad)
$\Delta\theta_r(\tau)$	Defined as $\theta_r(t_2) - \theta_r(t_1)$ (rad)
$\theta_d(s)$	Laplace transform of $\theta_d(t)$
$\theta_r(s)$	Laplace transform of $\theta_r(t)$
λ	Wavelength (meters)
ξ	Loop damping factor
σ_A^2	Phase variance matrix of a single reference array
σ_B^2	Phase variance matrix of a sequential array
σ_e^2	Variance of the measured laser field spectrum due to external noise
σ_{nm}^2	Phase variance between the nth and mth laser
σ_{0lmin}^2	Minimum laser differential phase variance for the basic two-laser loop

ϕ	Constant portion of phase (rad)
$\Delta\phi$	Phase step in the modulated reference phase (rad)
$\phi_n(t)$	Phase of the nth laser (rad)
$\phi_d(t)$	Laser differential phase (rad)
$\phi_r(t)$	Reference phase (rad)
$\psi(t)$	Phase error ($=\phi_r(t) - \phi_d(t)$) (rad)
$\Psi(s)$	Laplace transform of $\psi(t)$
ω	Radian frequency (rad/sec)
ω_n	Loop natural frequency (rad/sec)
$\Delta\omega_H$	Hold-in frequency range (rad/sec)
$\Delta\omega_L$	Lock-in frequency range (rad/sec)
$\Delta\omega_P$	Pull-in frequency range (rad/sec)
$\Delta\omega_S$	Frequency step limit (rad/sec)

Abstract

This paper presents design considerations and fundamental performance limitations of phase-lock control loops which are used to coherently combine a specified array of lasers. The control problem is first investigated in a "two-laser" control loop designed to lock the differential frequency/phase between the two lasers to a specified reference frequency. An optical heterodyne measurement configuration is used to determine the differential frequency and phase between the laser pair. An error voltage related to error between the desired frequency/phase (i.e., the rf reference) and the measured optical differential frequency/phase is filtered and used to frequency modulate one of the lasers (by electronically changing the effective cavity length) in an attempt to null the error. An integro-differential equation, valid for the linearized operating region of the loop is derived in terms of the specified (desired) phase control, the heterodyne measurement noise, and the various laser phase noises (instabilities). The power spectrum of the laser phase noise has two components: one due to quantum limitations (proportional to $1/f^2$) and the other due to random thermal and acoustical vibrations (proportional to $1/f^4$). The solution of the integro-differential equation results in an expression for the phase

error variance (the phase deviation between the two lasers) in terms of the closed-loop equivalent noise bandwidth of the system, W_H . The variance involves three terms: the first is proportional to $\Delta f_e / W_H^2$ where Δf_e is the linewidth of the combined laser fields due to external noise; the second is proportional to $\Delta f_q / W_H$ where Δf_q is the combined quantum limited laser field linewidth; while the third, due to measurement noise, is proportional to $hf_0 W_H$ where hf_0 is the energy of a detected photon. The conflicting effects of W_H on the terms in the phase error variance indicate that some optimization of W_H is desirable. In addition to noise effects, the relationship between the error voltage filters' characteristics and W_H and other system performance parameters such as loop acquisition time, frequency pull-in range and steady state error is examined. A design example using a CO_2 waveguide laser paired with a relatively stable, conventional CO_2 laser was presented and found to have an rms phase deviation between the two lasers of less than .1 radian and a lock up time of no more than 1 μ sec. The basic pairwise control model is then used to develop control configurations for the phase coherent control of the laser array. Two configurations are presented: (1) all lasers are compared pairwise to the same reference laser and (2) each laser is locked pairwise in sequence across the array. The resulting implications of system complexity and potential relative phase errors across the array are discussed.

PHASE-LOCK CONTROL CONSIDERATIONS
FOR MULTIPLE, COHERENTLY
COMBINED LASERS

I. Introduction

A well-known method of generating periodic, optical pulse trains with high peak powers and extremely narrow pulses is the mode-locked laser (Ref 1:256-266). However, the modulation characteristics are largely dependent on the laser's cavity parameters. For instance, the pulse repetition rate of a mode-locked laser is determined primarily by the cavity length. Thus, the modulation format is inflexible.

Conceptually, it is easy to think of each of the laser modes as being generated in individual laser cavities. So, a generalized concept of mode locking could be the coherent combination of the outputs of an array of single mode, but electronically phase controlled, lasers. Such a configuration has a potential modulation format that is much more flexible. For the special case of each of the individual lasers offset from the next by a constant frequency, such a configuration will result in the familiar mode-locked waveforms. More general phase control of the individual lasers, however, will allow the synthesis of other space-time field waveforms.

The key requirement for such a system is the precise control of the relative frequencies and phases of the individual lasers of the array. This paper presents design considerations and fundamental performance limitations of phase-lock feedback loops which are used to achieve the desired coherent laser combination.

The control problem is first investigated in a two-laser or "pairwise" control loop designed to lock the differential frequency/phase between the two lasers to a desired, controllable value. An integro-differential equation, valid for the linearized operating region of the loop, is derived in terms of the desired frequency/phase control, the laser phase instabilities, and other loop component noises and instabilities. Expressions for the power spectra of the various noises and instabilities are developed and used to solve the integro-differential equation for the phase error variance in terms of the closed-loop noise equivalent bandwidth of the system. The phase error variance expression can be used to determine the optimum, i.e., minimum variance, closed-loop bandwidth. In addition to noise effects, system performance parameters (such as loop acquisition time, frequency pull-in range and steady state error) are related to the loop filter characteristics and the closed-loop bandwidth for various desired control schemes (such as step and ramp changes in frequency). Other design considerations such as loop control methods, laser field detectors, laser frequency modulation and laser quiescent

frequency will also be discussed. A detailed design example for the two-laser control loop is presented to illustrate the effects of the various noise and control parameters on the overall phase-lock performance.

Finally, the basic pairwise control model is used to develop control configurations for the phase coherent control of a laser array. Two configurations are presented: (1) all lasers are compared pairwise to the same reference laser and (2) each laser is locked pairwise in sequence across the array. The resulting implications of system complexity and potential relative phase errors across the array are discussed. Other array design considerations (such as stability of the reference laser, laser gain bandwidth, and beam combination) are also discussed.

II. Two-Laser Control Loop

The phase control of an array of lasers will first be investigated in "pairwise" control loops designed to lock the differential phase between two lasers to a desired value. The array can then be constructed by proper combination of the basic pairwise units. Phase control is accomplished by using common phaselock techniques which will be briefly reviewed first.

Basic Phaselock Loop

The standard device for estimating the phase of a signal is the phaselock loop (PLL). It is motivated from Estimation Theory, where the maximum a posteriori estimate of a signal phase in white, Gaussian noise results in such a signal processor. Such a model is valid for the problem at hand (Ref 2: Chap. 5, p. 123). The basic form of the PLL is shown in Figure 1.

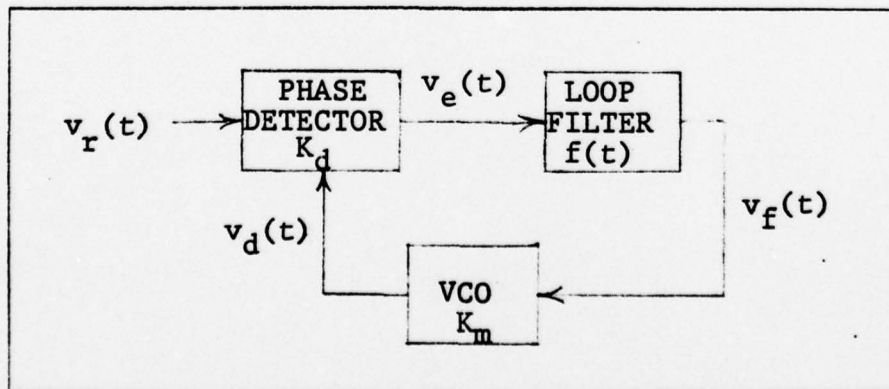


Figure 1. Basic Phaselock Loop

The loop input reference signal has the form:

$$v_r(t) = V_r \sin\phi_r(t) \quad (1)$$

where

$$\phi_r(t) = (2\pi f_d t + \phi_d) + \theta_r(t) \quad (2)$$

The first term, $(2\pi f_d t + \phi_d)$, is the constant portion of the reference phase and represents the voltage-controlled oscillator quiescent frequency. The second term, $\theta_r(t)$, is the modulated term and consists of two portions:

$$\theta_r(t) = \zeta(t) + \gamma_r(t) \quad (3)$$

where $\zeta(t)$ is the control modulation and $\gamma_r(t)$ is a zero mean random process representing the reference phase instabilities.

When the PLL is locked, the phase of the voltage controlled oscillator (VCO) is (ideally) equal to that of the input signal. The VCO output signal then has the form:

$$v_d(t) = V_d \cos\phi_d(t) \quad (4)$$

where

$$\phi_d(t) = (2\pi f_d t + \phi_d) + \theta_d(t) \quad (5)$$

The VCO signal also consists of a constant, quiescent phase term, $(2\pi f_d t + \phi_d)$, and a modulated term, $\theta_d(t)$.

If the phase detector (PD) is assumed to be linear, its output, called the phase error signal, is proportional to the difference between its two inputs times a phase detector gain K_d ,

$$v_e(t) = \mu K_d(\phi_r(t) - \phi_d(t)) \quad (6)$$

or cancelling the VCO quiescent phase term,

$$v_e(t) = \mu K_d(\theta_r(t) - \theta_d(t)) \quad (7)$$

where μ is the linear proportionality constant.

The phase error signal is filtered by a loop filter, $f(t)$, which helps determine the noise and dynamic performance of the loop. The filtered error signal is

$$v_f(t) = v_e(t) * f(t) = \int_{-\infty}^{\infty} v_e(u) f(t-u) du \quad (8)$$

The frequency of the VCO is controlled by the filtered error signal. The frequency deviation from the quiescent frequency is

$$\dot{\theta}_d(t) = 2\pi K_m v_f(t) \quad (9)$$

where K_m is the VCO gain in Hz/volt. It is convenient to express these results in the frequency domain. Taking the Laplace transforms of Eqs (7) through (9) gives respectively

$$V_e(s) = \mu K_d(\theta_r(s) - \theta_d(s)) \quad (10)$$

$$V_f(s) = V_e(s)F(s) \quad (11)$$

and

$$\theta_d(s) = \frac{K_m V_f(s)}{s} \quad (12)$$

Manipulation of these equations gives the basic PLL loop parameter

$$H(s) \equiv \frac{\theta_d(s)}{\theta_r(s)} = \frac{KF(s)}{s + KF(s)} \quad (13)$$

and

$$1-H(s) = \frac{\theta_r(s) - \theta_d(s)}{\theta_r(s)} = \frac{s}{s + KF(s)} \quad (14)$$

where $K = \mu K_m K_d$. The function $H(s)$ is called the closed-loop transfer function of the linear loop model. Thus, the PLL can equivalently be modeled as a simple linear filter, where the impulse response is $h(t) = L^{-1}[H(s)]$, as shown in Figure 2. The results for the basic PLL will now be used to solve the two-laser phase lock.

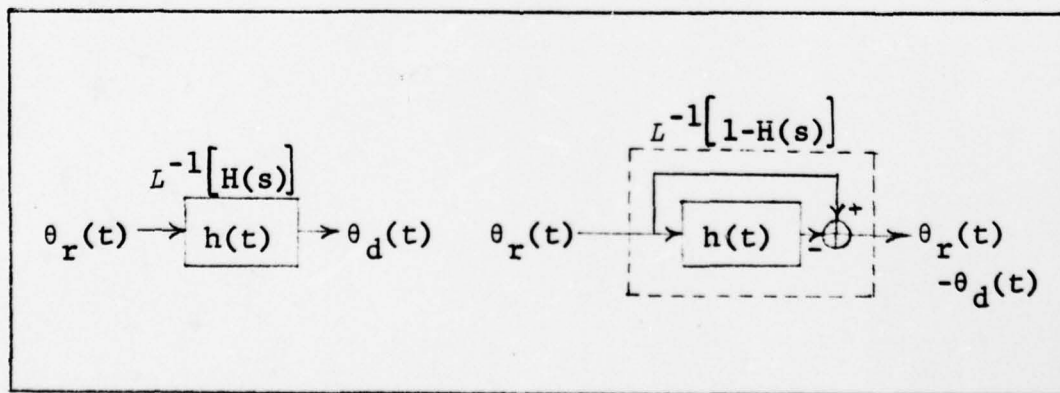


Figure 2. Equivalent Linear Filter Model of the Phaselock Loop

Pairwise Laser Phaselock

Ideally, two lasers could be placed in phaselock by letting the output field of one laser be the PLL input signal and letting the other, its frequency being voltage adjustable, act as the VCO. Unfortunately, this scheme is not feasible since there are no direct detectors for laser field, $E(\vec{r}, t)$. They all detect the intensity or power density of the field, $|E(\vec{r}, t)|^2$, thus losing all phase information. The extremely high laser frequencies, on the order of 10^{14} Hz, also present difficult problems.

To circumvent these problems, a common procedure is to sum the output fields of the two lasers into a single detector. The output of the detector will include a signal with a phase equal to the difference of the laser phases plus a low frequency term. The phase difference or "beat frequency" is more readily handled by available electronics. Typically, one laser has a very stable phase so that the phase instabilities of the other can be examined (Ref 3:509).

Another reason this procedure is so attractive is that excellent noise performance can be obtained with very simple post-detector processing. This technique is called heterodyne detection, the results of which are examined in Appendix A.

The basic PLL of Figure 1 can now be adapted to lock the phase difference between two lasers to a reference phase, as shown in Figure 3. The entire laser pair and

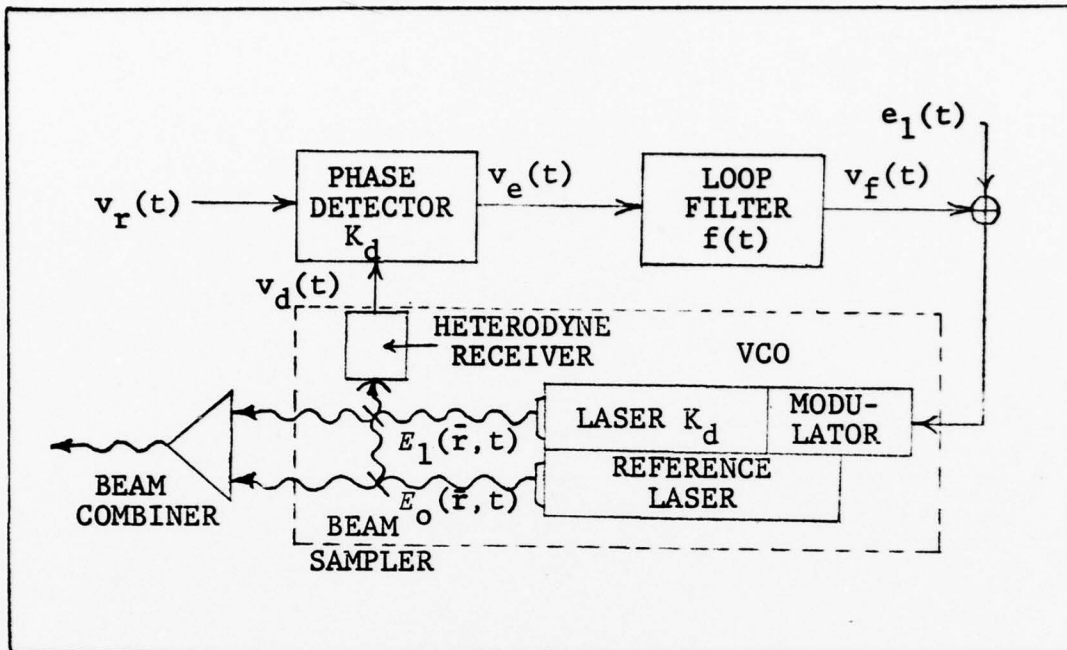


Figure 3. Two-Laser Differential Phase Control Loop

detector combination acts as the VCO. The filtered error voltage modulates the frequency of one laser only, but this is translated to a modulation in the differential phase seen at the detector. The voltage $e_1(t)$ is an analog control signal the uses of which will be discussed later. The important aspect of the two-laser loop is that the differential phase between the two lasers is locked to a reference phase; the absolute phase of the laser pair remains uncontrolled except by the nature of the lasers themselves and thus is free to fluctuate.

VCO Output. It will be assumed that the optics sampling the laser fields are aligned such that the beams fall collinearly upon the detector and that the fields are planar with

constant amplitudes (see Appendix A). Thus the incident fields for the reference and modulated lasers are respectively:

$$E_0(\bar{r}, t) = A_0 \cos \phi_0(t) = A_0 \operatorname{Re} \left[e^{j\phi_0(t)} \right] \quad (15)$$

$$E_1(\bar{r}, t) = A_1 \cos \phi_1(t) = A_1 \operatorname{Re} \left[e^{j\phi_1(t)} \right] \quad (16)$$

In this paper the $\operatorname{Re}[\]$ will be understood when using the complex envelope (exponential) notation. Thus the fields are written as

$$E_0(\bar{r}, t) = A_0 e^{j\phi_0(t)} \quad (17)$$

and

$$E_1(\bar{r}, t) = A_1 e^{j\phi_1(t)} \quad (18)$$

respectively. The planar assumption is reasonable if the detector is perpendicular to the beam at the beam waist, if the detector is curved to fit the curvature of the field, or, as is most likely, if the detector is small compared to the radius of curvature of the field. The constant amplitude assumption is a reasonable result of the nature of the laser instabilities if interest is primarily in the field frequency spectrum. This is discussed further in the opening paragraphs of Appendix B.

The phase of the reference laser is

$$\phi_0(t) = (2\pi f_0 t + \phi_0) + \gamma_0(t) \quad (19)$$

where $(2\pi f_0 t + \phi_0)$ is the operating phase and $\gamma_0(t)$ is a zero mean, Gaussian random process describing the measurable reference laser instabilities. Its statistical description is derived in detail in Appendix B. Since this laser is not modulated, f_0 is always the quiescent frequency f_{0q} , that is,

$$f_0 \equiv f_{0q} \quad (20)$$

The phase of the modulated laser is

$$\phi_1(t) = (2\pi f_1 t + \phi_1) + \gamma_1(t) \quad (21)$$

where $(2\pi f_1 t + \phi_1)$ is the operating phase and $\gamma_1(t)$ is again a zero mean, Gaussian random process representing that laser's instabilities (Appendix B). More specifically, the operating frequency f_1 , consists of a constant quiescent frequency f_{1q} portion and a portion modulated by the filtered error and control signals. Frequency modulation of lasers for control applications is discussed briefly in Appendix C. From Eq (C-17), the instantaneous frequency of the modulated laser is

$$\dot{\phi}_1(t) = 2\pi [f_{1q} + K_m(v_f(t) + e_1(t))] + \dot{\gamma}_1(t) \quad (22)$$

where K_m is the modulator gain in Hz per volt.

The two laser fields of Eqs (17) and (18) are added on the detector surface such that without loss of generality, $A_0 \gg A_1$. (The reverse $A_1 \gg A_0$ could also be true but would be included in the following with a simple change of

subscripts.) The output of the heterodyne receiver (HR) is, from Eqs (A-13) and (A-16) in Appendix A,

$$v_d(t) = V_d \cos \phi_d(t) + n(t) \quad (23)$$

where $n(t)$ is a zero mean random process describing the HR noise. The phase is

$$\phi_d(t) = \phi_1(t) - \phi_0(t) \quad (24)$$

$$= 2\pi f_d t + \phi_d + \theta_d(t) \quad (25)$$

where

$$f_d = f_{1q} - f_{0q} \quad (26)$$

and

$$\phi_d = \phi_1 - \phi_0 \quad (27)$$

The phase modulation portion is

$$\dot{\theta}_d(t) = 2\pi K_m (v_f(t) + e_1(t)) + \dot{\gamma}_d(t) \quad (28)$$

where

$$\gamma_d(t) = \gamma_1(t) - \gamma_0(t) \quad (29)$$

Eq (28) is the same as Eq (9) of the basic PLL results but includes a control signal and an instability term. The HR noise in Eq (23) arises from the fundamental quantum nature of the optical fields and should not be confused with the noise arising from the laser phase instabilities.

Using the quadrature component representation of the HR noise, as outlined in Appendix D, and assuming that the noise spectrum is symmetric on the VCO quiescent frequency f_d , Eq (23) can be rewritten as

$$v_d(t) = V_d \cos \phi_d(t) + n_c(t) \cos(\omega_d t + \phi_d) + n_s(t) \sin(\omega_d t + \phi_d) \quad (30)$$

where $n_c(t)$ and $n_s(t)$ are the in-phase and quadrature components of the noise $n(t)$, respectively. Eq (30) is the VCO output.

Loop Reference Input. The loop reference signal remains the same as that of the basic loop given in Eqs (1) through (3). All derivations will be made with respect to the laser differential (VCO) quiescent frequency, f_d .

Phase Detector Output. The reference and VCO signals, as seen in Figure 2, meet in a phase detector (PD). The PD will be modeled as a multiplier with double frequency components removed (Ref 4:58). The output of the PD, called the error signal, is then

$$v_e(t) = K_d L_p [v_r(t) v_d(t)] \quad (31)$$

where K_d is the PD gain and $L_p []$ denotes the low pass portion of the quantity in brackets. Substituting Eqs (1) and (30) into the above equation results in

$$v_e(t) = \frac{K_d V_r V_d}{2} (\sin \psi(t) + n'(t)) \quad (32)$$

where

$$n'(t) = \frac{1}{V_d} [n_c(t) \sin \theta_r(t) + n_s(t) \cos \theta_r(t)] \quad (33)$$

and

$$\psi(t) = \phi_r(t) - \phi_d(t) = \theta_r(t) - \theta_d(t) \quad (34)$$

The variable $\psi(t)$ is called the loop phase error. As seen in Eq (33) the noise due to the HR is independent of the loop phase error. Eq (32) is the equivalent of Eq (7) in the basic PLL results where $\mu = V_r V_d / 2$, but is nonlinear in $\psi(t)$ and contains detector noise.

Loop Filter Output. Referring again to Figure 2, the error signal is now passed through a loop filter $f(t)$ which gives a filtered error voltage of

$$v_f(t) = \frac{K_d V_r V_d}{2} (\sin \psi(t) + n'(t)) * f(t) \quad (35)$$

This is equivalent to Eq (8) of the basic PLL results.

Loop Equation. The filtered error voltage plus a control voltage is next fed back into the frequency modulator of the modulated laser changing its output frequency as described in Eq (22). The instantaneous frequency of the VCO output is, from Eqs (25) and (28):

$$\dot{\phi}_d(t) = 2\pi [f_d + K_m (v_f(t) + e_1(t))] + \dot{\gamma}_d(t) \quad (36)$$

Substituting into this expression the results derived for filtered error signal, Eq (35), gives

$$\dot{\phi}_d(t) = 2\pi f_d + \left[K(\sin\psi(t) + n'(t)) * f(t) \right] + 2\pi K_m e_1(t) + \dot{\gamma}_d(t) \quad (37)$$

where

$$K = \pi K_m K_d V_r V_d \quad (38)$$

Finally, using Eq (34), the nonlinear stochastic integro-differential equation for the loop phase error is

$$\dot{\psi}(t) = \dot{\theta}_r(t) - K(\sin\psi(t) + n'(t)) * f(t) - 2\pi K_m e_1(t) - \dot{\gamma}_d(t) \quad (39)$$

This equation will be linearized by assuming that $\psi(t)$ is small (less than 1 radian) so that $\sin\psi(t) \approx \psi(t)$. Additionally, converting this equation into the frequency domain by taking the Laplace transform yields

$$\Psi(s) = \Theta_r(s) - \Gamma_d(s) - \frac{1}{s} \left[KF(s)(\Psi(s) + N'(s)) + 2\pi K_m E_1(s) \right] \quad (40)$$

(It is assumed that the transform of the sample functions of the random processes exist.) This linearized version of the integro-differential equation is graphically depicted in Figure 4.

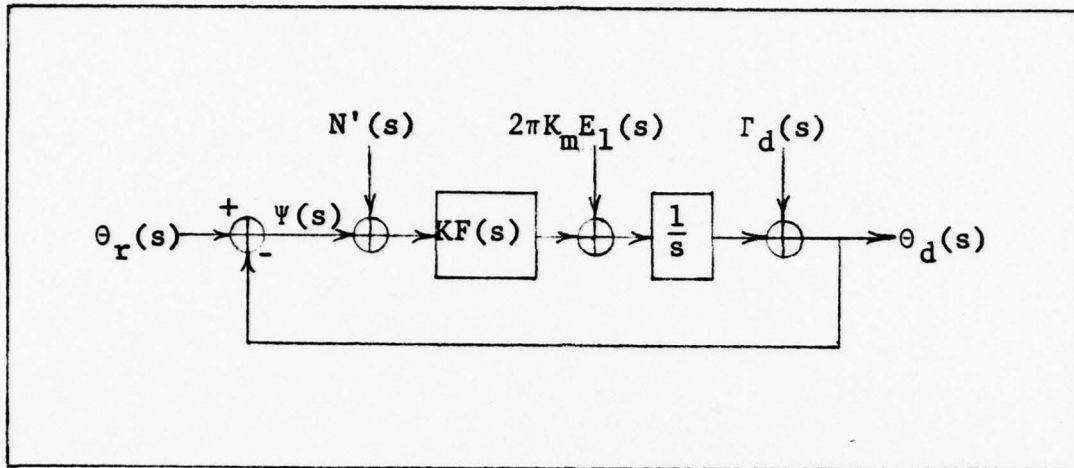


Figure 4. Linear Two-Laser Phaselock Loop Model

Solving for $\Psi(s)$ gives

$$\Psi(s) = \left[\frac{s}{s+KF(s)} \right] (\theta_r(s) - \Gamma_d(s)) - \left[\frac{1}{s+KF(s)} \right] 2\pi K_m E_1(s) - \left[\frac{KF(s)}{s+KF(s)} \right] N'(s) \quad (41)$$

This is the loop phase error between the laser differential phase and the desired reference phase. It will become important when considering the modulated, steady state response of the system in a later section.

In considering an array of phase locked lasers, of primary concern is the laser differential phase $\phi_d(t)$. Since $\phi_d(t) = (2\pi f_d t + \phi_d) + \theta_d(t)$, it is sufficient to know only the modulated phase, $\theta_d(t)$. Substituting $\theta_r(s) - \theta_d(s)$ for $\Psi(s)$ (from Eq (34)) and solving for $\theta_d(s)$ gives

$$\theta_d(s) = \left[\frac{1}{s+KF(s)} \right] 2\pi K_m E_1(s) + \left[\frac{s}{s+KF(s)} \right] \Gamma_d(s) + \left[\frac{KF(s)}{s+KF(s)} \right] (N'(s) + \theta_r(s)) \quad (42)$$

The laser differential phase error can thus be obtained by passing the various noise, instability, and control processes through a set of linear filters. Eq (42) is shown graphically in Figure 5 for both Laplace and time domains. From Eq (3), the transform of the reference modulated phase is

$$\theta_r(s) = \zeta(s) + \Gamma_r(s) \quad (43)$$

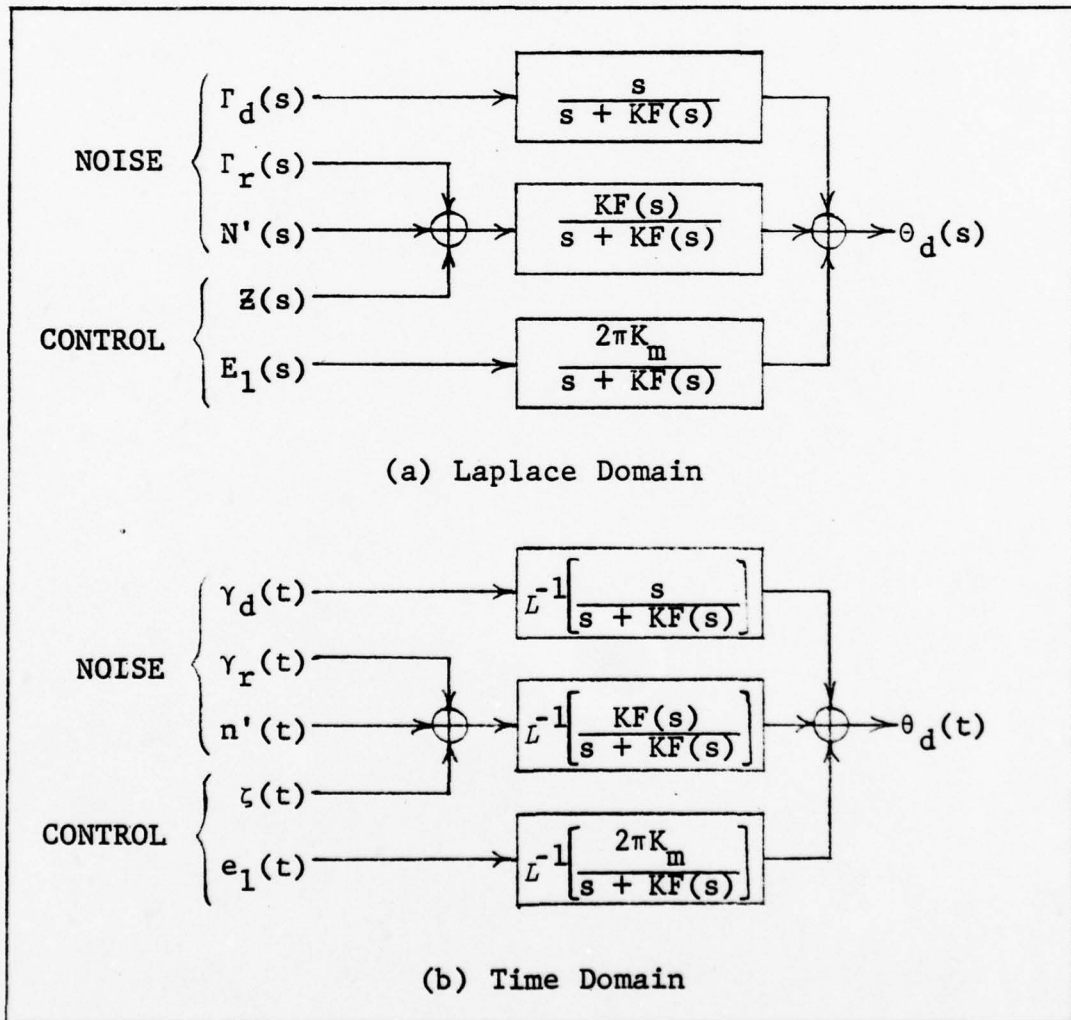


Figure 5. Equivalent Linear Filter Model of the Two-Laser Phaselock Loop for (a) Laplace and (b) Time Domains

To find the mean and variance of the laser differential phase error, the statistics of the noises and instabilities and the nature of the control modulation and control signals must be known. A first and second moment description of the noises and instabilities will be discussed next.

Statistical Description of Loop Noise Sources

There are three sources of noise preventing a steady value of laser differential phase. They are the loop reference phase instabilities, the individual laser phase instabilities, and the heterodyne receiver noise. A second moment model for each will be presented in this section.

Loop Reference Instabilities. As defined in Eq (3), the phase modulation of the loop reference phase consists of a control modulation component $\xi(t)$ and an instability component $\gamma_r(t)$. It will be assumed that the reference phase is very stable with respect to the other noises in the system, that is, $\gamma_r(t) \approx 0$. The phase modulation term thus consists only of the deterministic control term so that the mean and spectrum are

$$E[\theta_r(t)] = \zeta(t) \quad (44)$$

and

$$S_{\theta_r}(f) = S_{\gamma_r}(f) = 0 \quad (45)$$

(All power spectral densities in this paper are the Fourier

transform of the covariance of the particular stationary process, not the autocorrelation.)

Laser Phase Instabilities. As defined in Eq (29), the laser differential phase instability is due to the instabilities of both the reference and modulated lasers. The mean and power spectral density of the measured laser instabilities are derived in Appendix B. From Eq (B-8), the laser instabilities are zero mean, thus

$$E[\gamma_d(t)] = 0 \quad (46)$$

It will further be assumed that the instabilities in each laser are statistically independent, which is reasonable if they are in their own thermally and acoustically isolated cavities. Using this assumption, the spectrum of the difference is the sum of the individual spectra. Thus from Eq (B-49) is obtained

$$S_{\gamma_d}(f) = \frac{1}{f^2} \left[(\alpha_o + \alpha_1) + \frac{\beta_o f_{co}}{f_{co}^2 + f^2} + \frac{\beta_1 f_{c1}}{f_{c1}^2 + f^2} \right] \quad (47)$$

where

$$\alpha = \frac{\Delta f_q}{2\pi} \quad (48)$$

and

$$\beta = \frac{\sigma_e^2}{\pi} = \frac{\Delta f_e^2}{8\pi \ln 2} \quad (49)$$

The variable Δf_q is the full width at half maximum (FWHM) of the quantum limit of the laser field line width and Δf_e

is the FWHM of the laser field line width due to all other sources, primarily by thermal and acoustic fluctuations (Ref 1:304). The variables f_{c0} and f_{c1} are mathematically expedient cutoff frequencies and are explained in detail in the appendix.

Thus the power spectrum of the laser differential phase noise has two components: one due to quantum limitations (proportional to $1/f^2$) and the other due to random external vibrations (proportional to $1/f^4$).

Heterodyne Receiver Noise. The loop phase noise due to the HR is from Eq (33)

$$n'(t) = \frac{1}{V_d} [n_c(t) \sin \theta_r(t) + n_s(t) \cos \theta_r(t)] \quad (33)$$

Drawing freely from the properties of narrowband noise listed in Appendix D, the mean of $n'(t)$ using Eq (D-2) is simply

$$E[n'(t)] = 0 \quad (50)$$

The autocorrelation of $n'(t)$ is

$$R_{n'}(t_2, t_1) = E[n'(t_2)n'(t_1)] \quad (51)$$

which when expanded becomes

$$R_{n'}(t_2, t_1) = \frac{1}{V_d^2} \{ R_{n_c}(\tau) E[\cos(\theta_r(t_2) - \theta_r(t_1))] + R_{n_s}(\tau) E[\sin(\theta_r(t_2) + \theta_r(t_1))] \} \quad (52)$$

where $\tau = t_2 - t_1$. Since the noise spectrum of $n(t)$, $S_n(f)$,

is assumed to be symmetric about f_d (Eqs (A-14) and (A-17)), the cross correlation between $n_c(t)$ and $n_s(t)$ is zero and Eq (52) reduces to

$$R_{n'}(t_2, t_1) = \frac{1}{V_d^2} R_{n_c}(\tau) E[\cos \Delta\theta_r(\tau)] \quad (53)$$

where

$$\Delta\theta_r(\tau) = \theta_r(t_2) - \theta_r(t_1) \quad (54)$$

$$= \zeta(t_2) - \zeta(t_1) + \gamma_r(t_2) - \gamma_r(t_1) \quad (55)$$

This result is strictly not stationary. However, recall that it was previously assumed that the reference is very stable so that $\gamma_r(t) \approx 0$. It is further assumed that the desired modulation $\zeta(t)$, will not change as fast as (will have a larger correlation time than) the other system processes. So for time intervals of interest it follows that

$$\Delta\theta_r(\tau) \approx 0 \quad (56)$$

so that

$$R_{n'}(t_2, t_1) = R_{n'}(\tau) = \frac{1}{V_d^2} R_{n_c}(\tau) \quad (57)$$

or finally

$$S_{n'}(f) = \frac{1}{V_d^2} S_{n_c}(f) \quad (58)$$

From the results of Appendix A (Eqs (A-14) and (A-17)) and

Appendix D (Eq (D-3)), the power spectrum of the loop noise due to the HR is then

$$S_{n'}(f) = \frac{q^2 \eta A_d A_o^2 R^2}{hf_o C_{01}^2 V_d^2} , \quad |f| \leq B_{01}/2 \quad (59)$$

where q is the charge of an electron, η the detector quantum efficiency in photo-electrons per photon, R is an effective HR resistance, A_d is the active area of the detector, and $1/C_{01}^2$ and B_{01} are the magnitude and bandwidth of the HR BPF transfer function respectively. Eq (59) can be reduced further by using the value for V_d stated in Eq (A-15) which when substituted gives

$$S_{n'}(f) = \frac{hf_o}{A_d A_1^2 \eta} , \quad |f| \leq B_{01}/2 \quad (60)$$

The power spectrum of the loop noise due to the HR is then proportional to the energy of a detected photon, hf_o .

With the statistical nature of the reference instability, laser instability, and HR noise now specified, the performance of the laser differential phase from Eq (42) can now be determined.

Steady State, Second Moment Description of the Laser Pair Differential Phase

Using the basic PLL transfer function of Eqs (13) and (14), Eq (42) can alternately be written in terms of the closed loop transfer function, $H(s)$, as

$$\theta_d(s) = \left[\frac{1-H(s)}{s} \right] 2\pi K_m E_1(s) + [1-H(s)] \Gamma_d(s) + [H(s)] (N'(s) + \theta_r(s)) \quad (61)$$

Since the exact nature of $F(s)$ need not be specified, this equation is more convenient to use in deriving expressions for the steady state mean and variance of $\theta_d(t)$. In this section, the mean will only be derived for the unmodulated case ($\zeta(t) = e_1(t) = 0$) since $F(s)$ must be known if there is modulation. The modulated steady state mean is discussed in the section on loop filter design. To simplify the problem, an equivalent model for $H(s)$ will be used.

Noise Equivalent Bandwidth Model of the Closed-Loop Transfer Function. The closed-loop transfer function is from Eq (13)

$$H(s) = \frac{KF(s)}{s+KF(s)} \quad (13)$$

For any loop filter $F(s)$ considered here, the following is true:

$$|H(0)|^2 = 1 \quad (62)$$

The noise equivalent bandwidth (NEB) of $H(s)$ is defined as an ideal low pass filter (LPF) with magnitude $|H(0)|^2$ and one sided bandwidth W_H whose area under the curve is the same as the area under $|H(s)|^2$ across the entire spectrum (Ref 5:33). That is

$$W_H = \frac{1}{4\pi j} \int_{-j\infty}^{j\infty} |H(s)|^2 ds \quad (63)$$

or in Fourier notation

$$W_H = \int_0^{\infty} |H(j2\pi f)|^2 df \quad (64)$$

This is shown graphically in Figure 6.

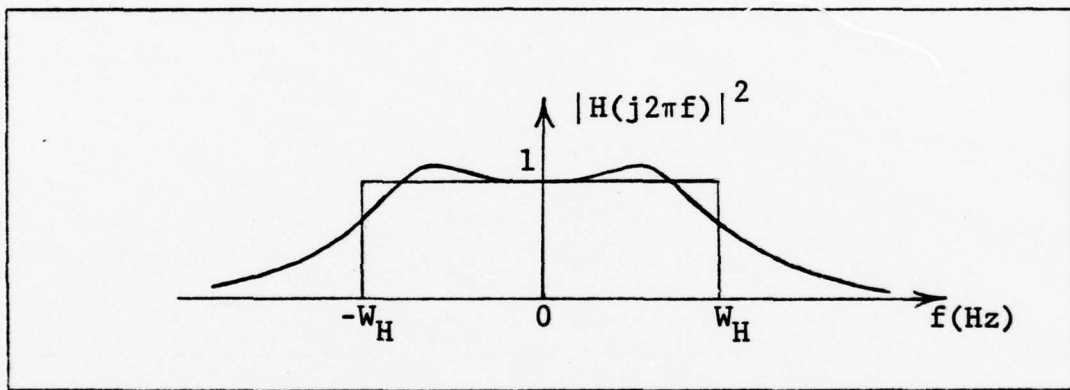


Figure 6. Noise Equivalent Bandwidth Model of the Closed Loop Transfer Function

The exact size of W_H will of course depend on the exact nature of $F(s)$. Although ideally $F(s)$ is only the loop filter which follows the PD in the loop (Figure 2), this assumes that no filtering occurs elsewhere in the loop. However, realistically, $F(s)$ includes contributions not only from the designed loop filter, but from every other component in the loop (e.g., the response time of the laser phase modulator and the HR BPF), thus the component with the

narrowest bandpass response will set the maximum limit on the value of W_H . In this model, the two dominate filtering sources are the designed filter and the HR BPF, the narrower of which will determine W_H .

Steady State Mean. The laser differential phase error is given by Eq (42). Using the expression for the expected value of laser phase noise Eq (46); HR noise, Eq (50); and loop reference phase modulation, Eq (44), the mean of the laser differential phase error is

$$E[\theta_d(s)] = \left[\frac{1}{s+KF(s)} \right] 2\pi K_m E_1(s) + \left[\frac{KF(s)}{s+KF(s)} \right] Z(s) \quad (65)$$

where

$$Z(s) = L[\zeta(t)] \quad (66)$$

If the system is unmodulated, that is $e_1(t) = \zeta(t) = 0$ then

$$E[\theta_d(t)] = E[\theta_d(s)] = 0 \quad (67)$$

and the constant phase between lasers, from Eqs (2) and (25) is

$$E[\phi_d(t)] = E[\phi_r(t)] = 2\pi f_d t + \phi_d \quad (68)$$

That is, the phase difference between the two lasers is equal to the loop reference phase when the system is unmodulated.

A similar procedure starting with Eq (41), results in a mean of the loop phase error of

$$E[\Psi(s)] = \left[\frac{s}{s+KF(s)} \right] Z(s) - \left[\frac{1}{s+KF(s)} \right] 2\pi K_m E_1(s) \quad (69)$$

Again, if the system is unmodulated, then

$$E[\psi(t)] = E[\Psi(s)] = 0 \quad (70)$$

which is the expected result from Eq (34) since

$$\psi(t) = \phi_r(t) - \phi_d(t) \quad (34)$$

As desired, the laser differential phase is matched on the average to the loop reference phase when the system is unmodulated. A measure of fluctuations away from this desired result is now required. This will be found in terms of variance from the mean.

Steady State Variance. Eq (61) can be slightly modified as

$$\theta_d(s) = [1-H(s)] \left(\frac{2\pi K_m E_1(s)}{s} + \Gamma_d(s) \right) + [H(s)] (N'(s) + \theta_r(s)) \quad (71)$$

This expression shows that the phase error is obtained by passing the HR noise and reference phase modulation through the filter $H(s)$ and the integrated control signal and laser instabilities through the filter $[1-H(s)]$. Using the NEB model of $H(s)$ and assuming that all the processes are

statistically independent and that $\zeta(t) = e_1(t) = 0$ (no modulation), the variance of the phase error is

$$\sigma_{01}^2 = 2 \int_0^{W_H} [S_{n_r}(f) + S_{\gamma_r}(f)] df + 2 \int_{W_H}^{\infty} S_{\gamma_d}(f) df \quad (72)$$

The two terms of this integral are illustrated in Figure 7 to aid in showing the effect of W_H on the resulting σ_{01}^2 .

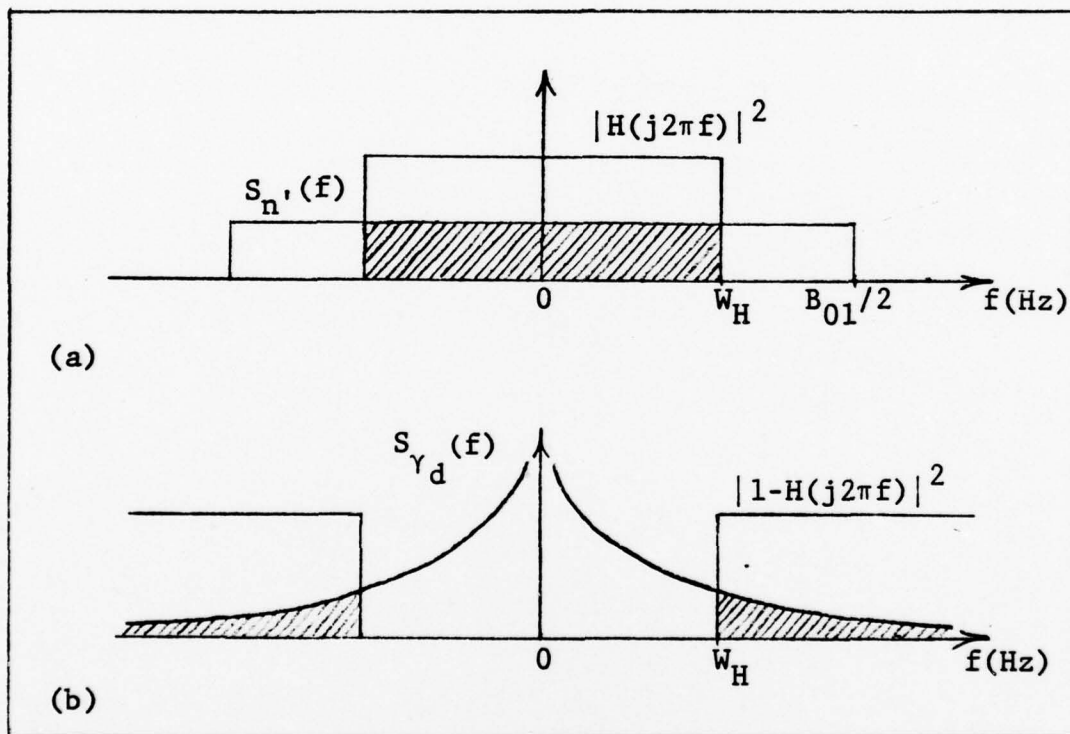


Figure 7. Graphical Representation of Contributions to the Laser Differential Phase Error Variance due to (a) the Heterodyne Receiver Noise and (b) the Lasers' Phase Instabilities

The total crosshatched area on the two graphs is the variance. In Figure 7a, as previously noted, $B_{01}/2$ by

definition can never be less than W_H . Thus from the point of view of the closed-loop transfer function, the HR noise $n'(t)$ is nearly white.

Using the values for the spectral densities of Eqs (45), (47), and (60) and integrating reduces Eq (72) to

$$\begin{aligned} \sigma_{01}^2 = & \frac{2hf_o W_H}{\eta A_d A_1^2} + \frac{2(\alpha_o + \alpha_1)}{W_H} + \frac{2\beta_1}{f_{c1}} \left[\frac{f_{c1}}{W_H} - \frac{\pi}{2} + \tan^{-1} \frac{W_H}{f_{c1}} \right] \\ & + \frac{2\beta_o}{f_{co}} \left[\frac{f_{co}}{W_H} - \frac{\pi}{2} + \tan^{-1} \frac{W_H}{f_{co}} \right] \end{aligned} \quad (73)$$

From Appendix B, f_{co} and f_{c1} , are arbitrarily small (experimentally less than 1 Hz (Ref 6:184)) so it is reasonable to assume that

$$\frac{W_H}{f_{co}} \gg 1 \quad (74)$$

and

$$\frac{W_H}{f_{c1}} \gg 1 \quad (75)$$

Using that result, the \tan^{-1} terms can be approximated by the first three terms of their power series as

$$\tan^{-1} \frac{W_H}{f_c} \approx \frac{\pi}{2} - \frac{f_c}{W_H} + \frac{f_c^2}{3W_H^2} \quad (76)$$

Substituting this approximation back into Eq (73) finally yields an expression for the laser differential phase error variance of

$$\sigma_{01}^2 = \hat{C}_1 W_H + \frac{\hat{C}_2}{W_H} + \frac{\hat{C}_3}{W_H^2} \quad (77)$$

where

$$\hat{C}_1 = \frac{2hf_o}{\eta A_d A_1^2} \quad (78)$$

$$\hat{C}_2 = 2(\alpha_o + \alpha_1) \quad (79)$$

and

$$\hat{C}_3 = \frac{2(\beta_o + \beta_1)}{3} \quad (80)$$

The variable \hat{C}_1 is proportional to the energy of a detected photon, hf_o ; \hat{C}_2 is proportional to Δf_q , the sum of the quantum limited laser field linewidths; and \hat{C}_3 is proportional to Δf_e , the sum of the laser field linewidths due to external effects. The conflicting effects of the closed-loop bandwidth on the terms in the phase error variance indicate that some optimization of W_H is desirable.

Two-Laser Loop Design Considerations

Several parameters are important when considering the two-laser loop performance. One measure of performance is the laser differential phase error variance which, as was shown in Eq (77), depends on the closed-loop bandwidth. This result, however, was based on the assumption that the

loop reference signal was perfectly stable. Reference instabilities must ultimately be considered in the loop variance performance.

Variance is not the only measure of performance. In addition, the loop must be able to accurately respond to the desired modulation schemes of the reference signal thus placing minimum standards on the loop filter design and the loop dynamic response. All of these design considerations will now be examined.

Minimum Phase Variance Bandwidth. To optimize the loop performance, the variance of the laser differential phase must be minimized. The expression for phase error variance is given by Eq (77) and a plot showing the effect of the three different terms is given in Figure 8.

To find W_H such that σ_{01}^2 is minimal, take the derivative of Eq (77) with respect to W_H and set it equal to zero. This leaves

$$0 = W_H^3 - \frac{\hat{C}_2}{\hat{C}_1} W_H - \frac{2\hat{C}_3}{\hat{C}_1} \quad (81)$$

Since \hat{C}_1 , \hat{C}_2 , \hat{C}_3 and W_H are all real, the only real solution to the cubic equation gives the minimum variance bandwidth as

$$W_{Hmin} = \sqrt[3]{\frac{\hat{C}_3}{\hat{C}_1} + \sqrt{\left(\frac{\hat{C}_3}{\hat{C}_1}\right)^2 - \left(\frac{\hat{C}_2}{3\hat{C}_1}\right)^3}} + \sqrt[3]{\frac{\hat{C}_3}{\hat{C}_1} - \sqrt{\left(\frac{\hat{C}_3}{\hat{C}_1}\right)^2 - \left(\frac{\hat{C}_2}{3\hat{C}_1}\right)^3}} \quad (82)$$

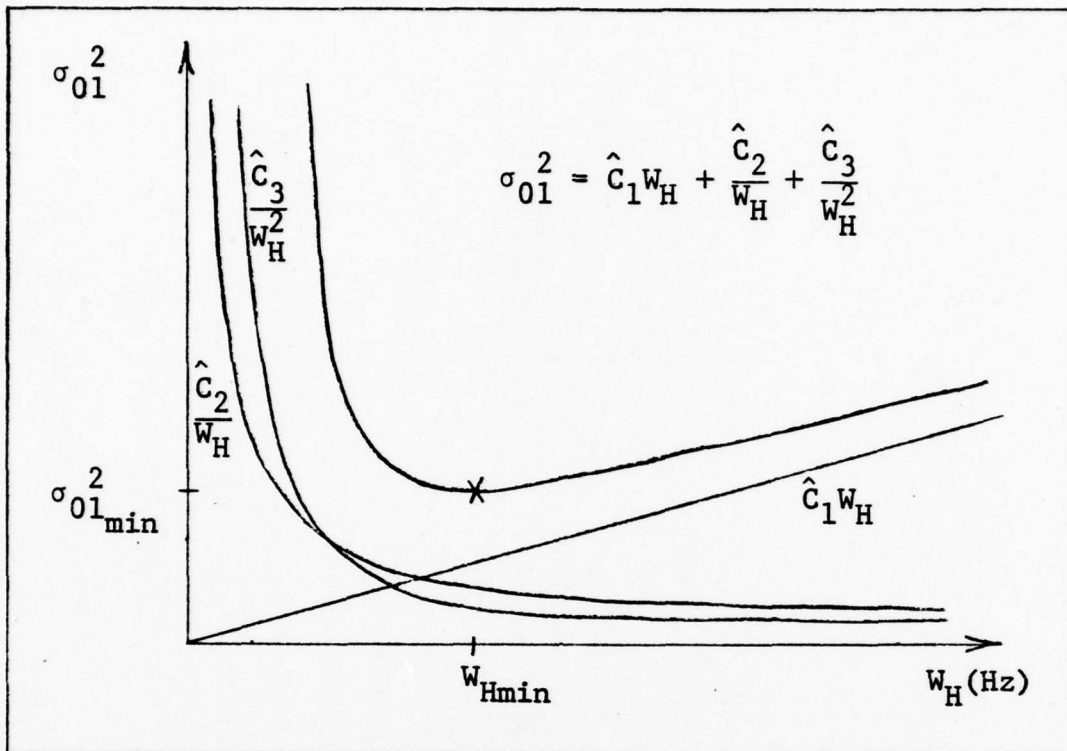


Figure 8. Closed Loop Bandwidth versus Laser Differential Phase Error Variance

If $\hat{C}_3^2 \gg \hat{C}_2^3$, which is typically the case since, for most lasers $\Delta f_e \gg \Delta f_q$ (Ref 6:181), then Eq (82) simplifies to

$$W_{Hmin} \approx \sqrt[3]{\frac{2\hat{C}_3}{\hat{C}_1}} \quad (83)$$

It is obvious from the examination of Figure 7, that if the actual bandwidth is less than W_{Hmin} the variance is limited by the laser phase instabilities (i.e., laser phase noise dominates). If W_H is greater than W_{Hmin} the variance is dominated by detector noise. Surprisingly, it will be shown that in many conceivable systems, $W_H < W_{Hmin}$ because W_{Hmin} is

very large and thus the variance is limited by the phase instabilities of the lasers and is independent of the HR measurement noise (see the numerical example in a later section).

Loop Filter Requirements. As stated earlier, $F(s)$ in Figure 2 actually includes all "filtering" by any component in the loop. It will be assumed that all of these components are controllable and thus $F(s)$ can be constructed as desired.

There are several loop filters that are commonly used in phase-lock loops (Ref 2:23). These are the first, second, and third order filters and are listed in Table I. The expressions for $H(s)$ and W_H were calculated using Eqs (13) and (64) respectively.

The steady state mean response of the laser differential phase error $\theta_d(t)$ for the modulated case can now be examined for each of the different loop filters under different control modulation schemes. The modulation schemes to be examined are listed in Table II in both Laplace and time domains. (Since each of the modulation schemes are causal, they are unique transform pairs.) The variable $\zeta(t)$ from Eq (3) is the control phase modulation of the loop reference phase and is in units of radians. The variable $e_1(t)$ is a control signal introduced after the loop filter and is measured in volts.

Once the filter and modulation scheme are known, the mean steady state response for the laser differential phase

Table I
Basic Parameters for First, Second and
Third Order Loop Filters

LOOP ORDER	LOOP FILTER TRANSFER FUNCTION $F(s)$	CLOSED LOOP TRANSFER FUNCTION $H(s)$	$1-H(s)$	NOISE EQUIVALENT BANDWIDTH W_H (Hz)
1	1	$\frac{K}{s+K}$	$\frac{s}{s+K}$	$\frac{K}{4}$
2	$1 + \frac{a}{s}$	$\frac{K(s+a)}{s^2 + K(s+a)}$	$\frac{s^2}{s^2 + K(s+a)}$	$\frac{K+a}{4}$
3	$1 + \frac{a}{s} + \frac{b}{s^2}$	$\frac{K(s^2+as+b)}{s^3 + K(s^2+as+b)}$	$\frac{s^3}{s^3 + K(s^2+as+b)}$	$\frac{K(aK + a^2 - b)}{4(aK - b)}$

Table II
Control Modulation Schemes in Temporal
and Laplace Representation

CONTROL VARIABLE	MODULATION SCHEME	TIME DOMAIN	LAPLACE REPRESENTATION
REFERENCE PHASE CONTROL MODULATION $\zeta(t)$ (radians)	Step in Phase	$\Delta\phi u(t)$	$\frac{\Delta\phi}{s}$
	Step in Frequency (Ramp in Phase)	$2\pi\Delta f t u(t)$	$\frac{2\pi\Delta f}{s^2}$
	Ramp in Frequency (Phase Acceleration)	$\frac{Dt^2}{2} u(t)$	$\frac{D}{s^3}$
MODULATION CONTROL SIGNAL $e_1(t)$ (volts)	Signal Step	$c_s u(t)$	$\frac{c_s}{s}$
	Signal Ramp	$c_r t u(t)$	$\frac{c_r}{s^2}$
	Signal Acceleration	$\frac{c_a t^2}{2} u(t)$	$\frac{c_a}{s^3}$

error can be determined. If it is the reference phase that is modulated then the loop phase error $\psi(t)$ becomes important. From Eq (34)

$$\psi(t) = \theta_r(t) - \theta_d(t) \quad (34)$$

and using Eq (44) (and the assumption that $\theta_r(t)$ and $\theta_d(t)$ are statistically independent) and exchanging terms gives

$$E[\theta_d(t)] = \zeta(t) - E[\psi(t)] \quad (84)$$

Thus the mean, steady state value for the laser differential phase error can be found by knowing the mean, steady state value for the loop phase error and the control modulation of the reference phase. For instance, if $\zeta(t)$ is a ramp in frequency, $\frac{Dt^2}{2}$, and the loop second order, then using Eq (69) and the final value theorem, the mean, steady state loop phase is

$$\lim_{t \rightarrow \infty} E[\psi(t)] = \lim_{s \rightarrow 0} sE[\Psi(s)] = \lim_{s \rightarrow 0} s \left[\frac{s^2 t}{s^2 + Ks + aK} \right] \frac{D}{s^3} \quad (85)$$

$$E[\psi(t)]_{ss} = D/aK \quad (\text{rad}) \quad (86)$$

Now utilizing Eq (84) the mean, steady state laser differential phase error is

$$E[\theta_d(t)]_{ss} = \frac{Dt^2}{2} - \frac{D}{aK} \quad (87)$$

That is, the loop will follow the frequency ramp (accelerating phase) but there will be a constant phase error offset of D/aK radians. This procedure is followed for all combinations of filter orders and reference phase modulations schemes and the results are summarized in Table III. Only the third order loop will follow accelerating phase with no constant phase offset. (The first order loop has a phase and frequency offset when trying to track accelerating phase and is not calculated.)

To calculate the mean steady state value for the laser differential phase when the control signal is modulated, Eq (65) is used. For example, if $e_1(t)$ is a voltage ramp, $C_r t$, and the loop is second order, then

$$\lim_{t \rightarrow \infty} [E \theta_d(t)] = \lim_{s \rightarrow 0} sE[\theta(s)] = \lim_{s \rightarrow 0} s \left[\frac{s}{s^2 + Ks + aK} \right] \frac{2\pi K_m C_r}{S^2} \quad (88)$$

$$E[\theta_d(t)]_{ss} = 2\pi K_m C_r / aK \quad (89)$$

Thus a constant phase offset between the lasers can be attained by use of the control signal $e_1(t)$. Results for other combinations of loop orders and control signal scheme are listed in Table III. (The first order loop has a frequency and ramp frequency offset when an accelerated control signal is applied and is not calculated.)

Actually, there appears to be no real advantage to using $e_1(t)$ instead of $\zeta(t)$ to control the laser differential

Table III
 Mean, Steady State Value of the Laser Differential Phase
 for Different Loop Orders and Modulation Schemes

$E[\theta_d(t)]_{ss}$ (radians)	$\zeta(t)$ (radians) ($e_1(t) = 0$)	$e_1(t)$ (volts) ($\zeta(t) = 0$)
LOOP ORDERS	$\Delta\phi u(t)$ $2\pi\Delta ft u(t)$ $\frac{Dt^2}{2} u(t)$	$c_s u(t)$ $c_r tu(t)$ $\frac{c_a t^2}{2} u(t)$
1	$\Delta\phi$ $2\pi\Delta ft - \frac{2\pi\Delta f}{K}$ ----	$\frac{2\pi K_m c_s}{K}$ $\frac{2\pi K_m c_r}{K} t$ *
2	$\Delta\phi$ $2\pi\Delta ft$ $\frac{Dt^2}{2} - \frac{D}{aK}$	0 $\frac{2\pi K_m c_r}{aK}$ $\frac{2\pi K_m c_a}{aK} t$ *
3	$\Delta\phi$ $2\pi\Delta ft$ $\frac{Dt^2}{2}$	0 0 $\frac{2\pi K_m c_a}{bK}$

* This term has an additional constant phase term of integration dependent on the initial conditions of $\theta_d(t)$ (at $t = 0$) which is not included in the table.

phase. The main use of the control signal $e_1(t)$ is in control of the modulated laser quiescent frequency f_{1q} . The VCO quiescent frequency is from Eq (26)

$$f_d = f_{1q} - f_{oq} \quad (26)$$

The frequency of the modulated laser from Eq (22) is

$$\dot{\phi}_1(t) = 2\pi [f_{1q} + K_m(v_f(t) + e_1(t))] + \dot{\gamma}_1(t) \quad (22)$$

If there is a dc component e_{1dc} , in addition to any modulated component $e_{1mod}(t)$ of the control signal then Eq (22) becomes

$$\dot{\phi}_1(t) = 2\pi [f'_{1q} + K_m(v_f(t) + e_{1mod}(t))] + \dot{\gamma}_1(t) \quad (90)$$

where

$$f'_{1q} = f_{1q} + K_m e_{1dc} \quad (91)$$

This will change the VCO quiescent frequency of Eq (26) accordingly.

The control signal could also be used to sweep the VCO frequency (using a voltage ramp) to "search" for the loop reference signal then release when the reference is acquired. Other dynamic effects of the loop will now be examined.

Loop Dynamic Effects. The loop filter, as shown previously, is important in determining the loop performance. First, the filter determines the closed-loop transfer function and resulting loop bandwidth (Table I). This in

turn influences the steady state variance of the laser differential phase error caused by the laser instabilities and detector noise. Second, the filter determines the steady state response of the loop to various modulation patterns (Table III). In addition to these steady state performances, the loop filter also determines the transient or dynamic response of the loop.

The most versatile filter, as seen in Table III, is the one resulting in a third-order loop. The exact behavior of a third-order loop is complex and difficult to obtain (Ref 2:72). However, it can be roughly contrasted with the second-order loop whose behavior is relatively well known. When a third-order loop is not initially locked to the loop reference phase, it is not as stable in its ability to acquire lock as the second-order loop. The second order results could in this case act as an upper bound ("best case") on the third-order loop performance (Ref 7:362). Once locked, however, the third-order can out perform the second-order loop, most notably in its ability to follow accelerating phase (frequency ramp) with no steady state phase error. In this case, second-order loop performance acts as a rough lower bound on third-order loop performance. More specific results must be obtained by computer simulation.

Some important performance equations for a second-order loop in a noiseless environment are listed in Table IV. Since they are valid for a noiseless environment, they represent the "best possible" performance in a noisy environment.

Table IV

Equations for Dynamic Performance of a Second-Order
Phase-Lock Loop in the Absence of Noise

TRACKING	
FREQUENCY STEP LIMIT	$\Delta\omega_s = 1.8 \omega_n (\xi + 1)$ rad/sec Ref (4:37)
HOLD-IN RANGE	$\Delta\omega_H = \pm \infty$ rad/sec Ref (7:359)
MAXIMUM TRACKING SWEEP RATE	$D_{\max} = \omega_n^2$ $= 2\omega_n^2$ (3 rd order loop) rad/sec ² Ref (2:55; 4:36; 7:360) Ref (2:66-72; 7:362)
ACQUISITION	
LOCK-IN FREQUENCY	$\Delta\omega_L = 2\xi\omega_n$ $= 2\omega_n (\xi + 0.6)$ rad/sec Ref (4:43) Ref (7:359)
LOCK-IN TIME	$T_L = 1.5/W_H$ $= \pi/\omega_n$ sec Ref (7:365) Ref (4:44)
PULL-IN FREQUENCY	$\Delta\omega_p = \pm \infty$ rad/sec Ref (2:51; 7:359)
PULL-IN TIME	$T_p = (\Delta\omega)^2 / 2\xi \omega_n^3$ sec Ref (4:46; 7:364)
MAXIMUM ACQUISITION SWEEP RATE	$R_{\max} = \omega_n^2 / 2$ $= a(4W_H - a)$ rad/sec ² Ref (4:47; 7:360) Ref (2:59)

These results are in terms of radian frequency ω (rad/sec) instead of f (Hz) since ω is typically used in the literature when dealing with dynamic feedback system behavior. The general relationship is $\omega = 2\pi f$. Some results utilize two, loop-parameter dependent variables called the natural frequency, ω_n , and the damping factor ξ . They are defined as follows (Ref 7:359):

$$\omega_n = \sqrt{aK} \quad (92)$$

$$\xi = \frac{1}{2} \sqrt{\frac{K}{a}} = \frac{K}{2\omega_n} \quad (93)$$

The natural frequency is the system phase error oscillation frequency in response to a step in the input reference frequency when there is no damping ($\xi = 0$). The damping factor is a measure of how quickly the oscillations attenuate as the loop acquires lock. Many of the expressions for the same parameter vary depending on the reference so all sources are also listed in the table.

The two main areas of transient behavior are tracking and acquisition. Tracking parameters assume that the loop is initially locked to the input reference phase. The hold-in range, $\Delta\omega_H$, is the maximum amount the reference frequency can deviate from the VCO quiescent frequency (HR output frequency) and have the loop remain locked. It is theoretically infinite for both second and third-order loops (Ref 7:358). Another important tracking parameter is the

frequency step limit, $\Delta\omega_s$. It is the maximum step in reference frequency below which the loop will not skip cycles. Cycle skipping occurs when the difference between the reference and VCO frequencies is large enough to create a differential frequency ("beat frequency") at the PD output.

Finally, the maximum reference frequency ramp that the loop will follow without dropping out of lock is called the maximum tracking sweep rate, D_{\max} (rad/sec²).

Acquisition parameters assume that the loop is not initially locked. The pull-in frequency, $\Delta\omega_p$, is the maximum amount the reference frequency can deviate from the VCO quiescent frequency and still permit the loop to converge to a locked state. This, like the hold-in range, is also theoretically infinite. As the loop converges on the reference frequency, the VCO frequency finally gets close enough to the reference frequency so that the loop stops skipping cycles and settles into the locked state. The range within which the loop ceases skipping cycles after pull-in is called the lock-in frequency, $\Delta\omega_L$. The associated times for the loop to pull-in and lock-in to a step change in reference frequency are respectively T_p and T_L . The pull-in time T_p includes only the time that the loop cycle-skips. The lock-in time T_L , is the time from the last cycle-skip until lock is acquired. The tracking frequency step limit $\Delta\omega_s$ is often equated with the acquisition lock-in frequency $\Delta\omega_L$ since the basic criterion in the definition of each is the maximum frequency difference below which the loop does not skip cycles.

It does not matter if this frequency difference occurs as a result of an input reference frequency step with the loop initially locked or as a result of pull-in with the loop attempting to acquire lock. This can readily be seen in the similarity of the expressions for $\Delta\omega_s$ and $\Delta\omega_L$ in Table IV. The lock-in time T_L thus applies to either case. Finally, the maximum frequency ramp that the loop can sweep and still acquire lock is called the maximum acquisition sweep rate, R_{\max} (rad/sec²).

It is important to note that these transient performance criterion may dominate simple noise considerations. If for example, W_H was chosen to minimize the phase error variance (Eq (82)), it might not be large enough to meet say the acquisition sweep rate demanded of the system.

Loop Reference Instability. The loop reference phase $\phi_r(t)$ was previously assumed to be perfectly stable, that is, the power spectrum of the phase instabilities was zero (Eq (45)). It is apparent from careful examination of Eq (42) or (61) that any loop reference phase instabilities $\gamma_r(t)$ will be passed by $H(s)$ and manifested in the laser differential phase error variance.

For example, if the power spectral density of the reference phase instabilities is nearly white it can be written as

$$S_{\gamma_r}(f) = \frac{N_r}{f_{cr}^2 + f^2} \quad (94)$$

where N_r is a constant and f_{cr} is a cutoff frequency which is very small (Ref 8:183). This expression is substituted back into Eq (72) and solved for phase error variance. The additional term that arises in the laser differential phase error variance σ_{01}^2 is

$$2 \int_0^{W_H} S_{\gamma_r}(f) df \quad (95)$$

which, after using the first two terms of the series for \tan^{-1} , becomes approximately

$$N_r \left(\frac{\pi}{f_{cr}} - \frac{2}{W_H} \right) \quad (96)$$

Not surprisingly, this term is reduced by making W_H small. A small W_H , as previously discussed can have an extremely detrimental effect on device flexibility. Thus the loop reference stability is extremely important in specific system design.

Other possible design considerations are mentioned in the conclusion of this paper. However, the effect of any given individual parameter (e.g., $F(s)$, $\gamma_d(t)$, $n'(t)$, $\zeta(t)$, etc.) on the overall laser differential phase $\theta_d(t)$ can readily be understood by careful examination of Figure 5 (Eq (42)). The steady state mean and variance of $\theta_d(t)$ due to unwanted fluctuations (detector noise, laser instabilities and reference instabilities) has been examined when the control inputs were zero. The steady state and dynamic changes

in $\theta_d(t)$ with various control inputs and filter designs were also examined. A design example for a potentially realizable two-laser control system will now be presented to illustrate the effects of the various parameters on the performance of the loop.

Numerical Design Example

The specific system to be examined here pairs a highly stable CO₂ reference laser with a highly adjustable CO₂ waveguide laser. CO₂ lasers were chosen because of their widespread use. The waveguide laser was chosen because it has a very wide gain bandwidth and thus can operate over a wide range of frequencies around the centerline frequency (Ref 9:1-33).

The transition of interest in this example is $\lambda = 10.6\mu$ which corresponds to:

$$f_o = 2.83 \times 10^{13} \text{ Hz} \quad (97)$$

The reference laser has the following characteristics:

$$\Delta f_{qo} = 6.28 \times 10^{-4} \text{ Hz} \quad (98)$$

and

$$\Delta f_{eo} = 7.77 \times 10^3 \text{ Hz} \quad (99)$$

The waveguide laser has the following characteristics:

$$P_1 = 2.4 \text{ watts} \quad (100a)$$

$$\alpha_l = .004 \text{ cm}^{-1} \quad (100b)$$

$$R_1 = .922 \quad (100c)$$

$$R_2 = 1.00 \quad (100d)$$

$$L = 20 \text{ cm} \quad (100e)$$

$$n = 1 \quad (100f)$$

and a useable gain linewidth (range over which the output frequency is adjustable and the laser power out does not drop below half its maximum value) of 7.00×10^8 Hz. From Eq (B-37),

$$\Delta f_{\text{cav}_1} = 2.85 \times 10^7 \text{ Hz} \quad (101)$$

It is further assumed that the waveguide laser is operating far enough above threshold so that $N_2/\Delta N \approx 1$. Thus from Eq (B-36),

$$\Delta f_{q1} = 2.00 \times 10^{-5} \text{ Hz} \quad (102)$$

The field spectrum linewidth of the waveguide laser (includes both quantum and external components) is measured as

$$\Delta f_{q1} + \Delta f_{e1} = 2.12 \times 10^7 \text{ Hz} \quad (103)$$

Thus

$$\Delta f_{e1} \approx 2.12 \times 10^7 \text{ Hz} \quad (104)$$

As is true here, most lasers' linewidths are dominated by external disturbances not quantum limitations. With the quantum and external linewidths for both lasers known, Eqs (48) and (49) can be used to find:

$$\alpha_0 = 1.00 \times 10^{-4} \text{ Hz} \quad (105a)$$

$$\alpha_1 = 3.18 \times 10^{-6} \text{ Hz} \quad (105b)$$

$$\beta_0 = 3.47 \times 10^6 \text{ Hz}^2 \quad (105c)$$

$$\beta_1 = 2.58 \times 10^{13} \text{ Hz}^2 \quad (105d)$$

Eqs (79) and (80) are then used to obtain

$$\hat{C}_2 = 2.06 \times 10^{-4} \text{ sec}^{-1} \quad (106)$$

and

$$\hat{C}_3 = 1.72 \times 10^{13} \text{ sec}^{-2} \quad (107)$$

Clearly, Δf_{e1} dominates in the term \hat{C}_3 . The HR samples 1×10^{-3} watts ($= A_d A_1^2$) and has a quantum efficiency of $\eta = 0.5$. Using Eq (78) it is found that

$$\hat{C}_1 = 7.51 \times 10^{-17} \text{ sec} \quad (108)$$

The reference signal is assumed to have no instabilities. If the HR BPF is designed to allow the frequency to range over the entire useable gain bandwidth, then B_{01} , must be greater than 7.00×10^8 Hz. Arbitrarily, B_{01} , is picked to be equal to that amount or:

$$B_{01} = 7.00 \times 10^8 \text{ Hz} \quad (109)$$

If it is assumed that the loop filter does not limit the bandpass of the loop, then W_H is at most $B_{01}/2$. The NEB, W_H , of the closed-loop transfer function reasonably must be somewhat less than that and is arbitrarily assumed to be

$$W_H = 4.15 \times 10^7 \text{ Hz} \quad (110)$$

Using the results for \hat{C}_1 , \hat{C}_2 , \hat{C}_3 and W_H the laser differential phase variance from Eq (77) is

$$\sigma_{01}^2 = 9.99 \times 10^{-3} \text{ rad}^2 \quad (111)$$

or a standard deviation of

$$\begin{aligned} \sigma_{01} &= .100 \text{ rad} \\ &= 5.75 \text{ degrees} \end{aligned} \quad (112)$$

This is a fairly good result. However, if W_H is decreased by only one order of magnitude to 4.15×10^6 Hz then the standard phase deviation will increase to $\sigma_{01} = 1$ rad (57.3 degrees). The minimum variance bandwidth using Eq (83) is

$$W_{Hmin} = 7.7 \times 10^9 \text{ Hz} \quad (113)$$

This is more than two orders of magnitude greater than the actual W_H thus the system is dominated by laser phase noise. The variance at W_{Hmin} is

$$\sigma_{01min}^2 = 8.68 \times 10^{-7} \text{ rad}^2 \quad (114)$$

or

$$\begin{aligned}\sigma_{01\min} &= .932 \text{ mrad} \\ &= .053 \text{ degrees}\end{aligned}\tag{115}$$

which is the best noise variance this particular loop can attain.

A second-order loop will be used in this example. A commonly employed compromise between stability and speed of response for a second-order system is to let (Ref 2:54)

$$\xi = .707\tag{116}$$

Using the expression for W_H of a second-order loop from Table I and Eq (93) to solve for K gives

$$K = 1.11 \times 10^8 \text{ sec}^{-1}\tag{117}$$

Again using Eq (93) gives

$$a = 5.53 \times 10^7 \text{ sec}^{-1}\tag{118}$$

and Eq (92) results then in

$$\omega_n = 7.83 \times 10^7 \text{ rad/sec}\tag{119}$$

The waveguide laser is modulated by a rectangular piezoelectric crystal 2.5 mm square by 25 mm long with a crystal constant of $d_{PE} = 225 \times 10^{-12}$ m/volt mounted on the rear mirror. Using these values in Eq (C-14) gives

$$K_m = 3.18 \times 10^5 \text{ Hz/volt}\tag{120}$$

Using Eq (38) leaves

$$K_d V_r V_d = 800 \text{ volts} \quad (121)$$

These three variables may be chosen arbitrarily as long as their product is the above constant. The detector output voltage amplitude V_d (Eq (A-15)) is most easily adjusted by varying the effective load resistance R . The loop reference voltage amplitude V_r is similarly adjusted. The variable K_d is the phase detector gain.

The transient performance of the loop is found by using the results of Table IV. The tracking frequency step limit is

$$\begin{aligned} \Delta\omega_s &= 2.41 \times 10^8 \text{ rad/sec} \\ &= 3.83 \times 10^7 \text{ Hz} \end{aligned} \quad (122)$$

The maximum tracking sweep rate is

$$\begin{aligned} D_{\max} &= 6.13 \times 10^{15} \text{ rad/sec}^2 \\ &= 9.76 \times 10^{14} \text{ sec}^{-2} \end{aligned} \quad (123)$$

The acquisition lock-in frequency is

$$\begin{aligned} \Delta\omega_L &= 2.05 \times 10^8 \text{ rad/sec} \\ &= 3.26 \times 10^7 \text{ Hz} \end{aligned} \quad (124)$$

As long as the changes in the reference input frequency are less than $\Delta\omega_L$ (or $\Delta\omega_s$) then the loop will have a lock-in time of no more than

$$T_L = 40 \text{ nsec} \quad (125)$$

If, however, the reference frequency changes by the full amount of useable laser gain linewidth, 7.00×10^8 Hz, then the pull-in time is

$$T_p = 722 \text{ nsec} \quad (126)$$

which is in addition to the lock-in time, giving a maximum time to lock of 762 nsec for the system. This is very good and could allow modulation on the order of msec with the loop still in lock. The maximum acquisition sweep rate is

$$\begin{aligned} R_{\max} &= 3.07 \times 10^{15} \text{ rad/sec}^2 \\ &= 4.88 \times 10^{14} \text{ sec}^{-2} \end{aligned} \quad (127)$$

There is, however, a steady state phase error if this second-order loop tracks a frequency ramp. If, for example, the tracking sweep rate is at its maximum allowable value for the loop ($D_{\max} = 6.13 \times 10^{15} \text{ rad/sec}^2$), the steady state phase error from Table III is 1 rad (57.3 degrees). A third-order loop must be used to eliminate this error.

This example has shown that even if one laser of the pair has a large field spectrum linewidth ($\sim 2.1 \times 10^7$ Hz) the loop can perform very well, with a standard deviation between the two-laser phases of less than 6 degrees and a maximum locking time of about 762 nsec. It is important to note that the system performance is limited by the laser phase instabilities (especially that of the waveguide laser)

and not by detector noise. The key elements in improving performance are to make W_H as large as possible and to make the lasers as stable as possible.

This completes the study of the two-laser control loop. The basic pairwise control model will now be used to develop control configurations for the phase coherent control of a laser array.

III. Laser Arrays

It is a relatively straightforward process to construct an array of phase locked lasers from the two-laser control loop. However, tradeoffs between equipment simplicity and laser differential phase performance can be made. Two array systems will be considered in terms of laser differential phase error variance. One consists of each laser in the array paired against the same reference laser and in the other each laser is paired against the next in sequence.

For this discussion the same quantities that were used in the two-laser problem will be subscripted with the appropriate number of the lasers in the array ($n = 0, 1, 2, \dots, N$). The reference laser is subscripted "0". Unless otherwise noted, it is assumed that the higher the laser number, the higher its operating frequency.

A critical assumption in any of the following arrays is that all of the loop reference signals are in phase with each other; that is, when all control voltages, $e_n(t)$, are zero, the phase difference between loop reference signals is precisely the same as between the respective laser pairs. Proper separation (control) of their phases then is mandatory for the coherent summation of all laser output phases. This requirement will be discussed later.

Single Reference Array

A single reference array is constructed of N modulated lasers each paired with the same single reference laser, in the same manner as discussed in the two-laser case, making a total of N lasers in the array. Thus there are N separate loops, one for each modulated laser as shown in Figure 9. The "nth laser pair" refers to the laser pair consisting of the reference laser and laser n. The "beam sampling optics" refers to the optics required to combine the laser output beams in the proper sequence and with the proper alignment into the detectors. The "beam combining optics" are those optics used to coherently add the output beams and direct the sum towards the target.

It will be assumed that the individual loops are uncoupled; that is, the performance of a given laser pair does not depend on the performance of any other laser pair. The variance of the laser differential phase error for the nth laser pair is then given according to Eq (77) as

$$\sigma_{0n}^2 = \hat{C}_{1n} W_{Hn} + \frac{\hat{C}_{2n}}{W_{Hn}} + \frac{\hat{C}_{3n}}{W_{Hn}^2} \quad (128)$$

The variables \hat{C}_{1n} , \hat{C}_{2n} , \hat{C}_{3n} and W_{Hn} are defined by Eqs (78), (79), (80), and (64) respectively. Since ultimately the system adds all laser beams to a single output, it is important to know the variance of phase differences among all the lasers in the array. To do this it is assumed that the noises and instabilities of all N lasers are statistically

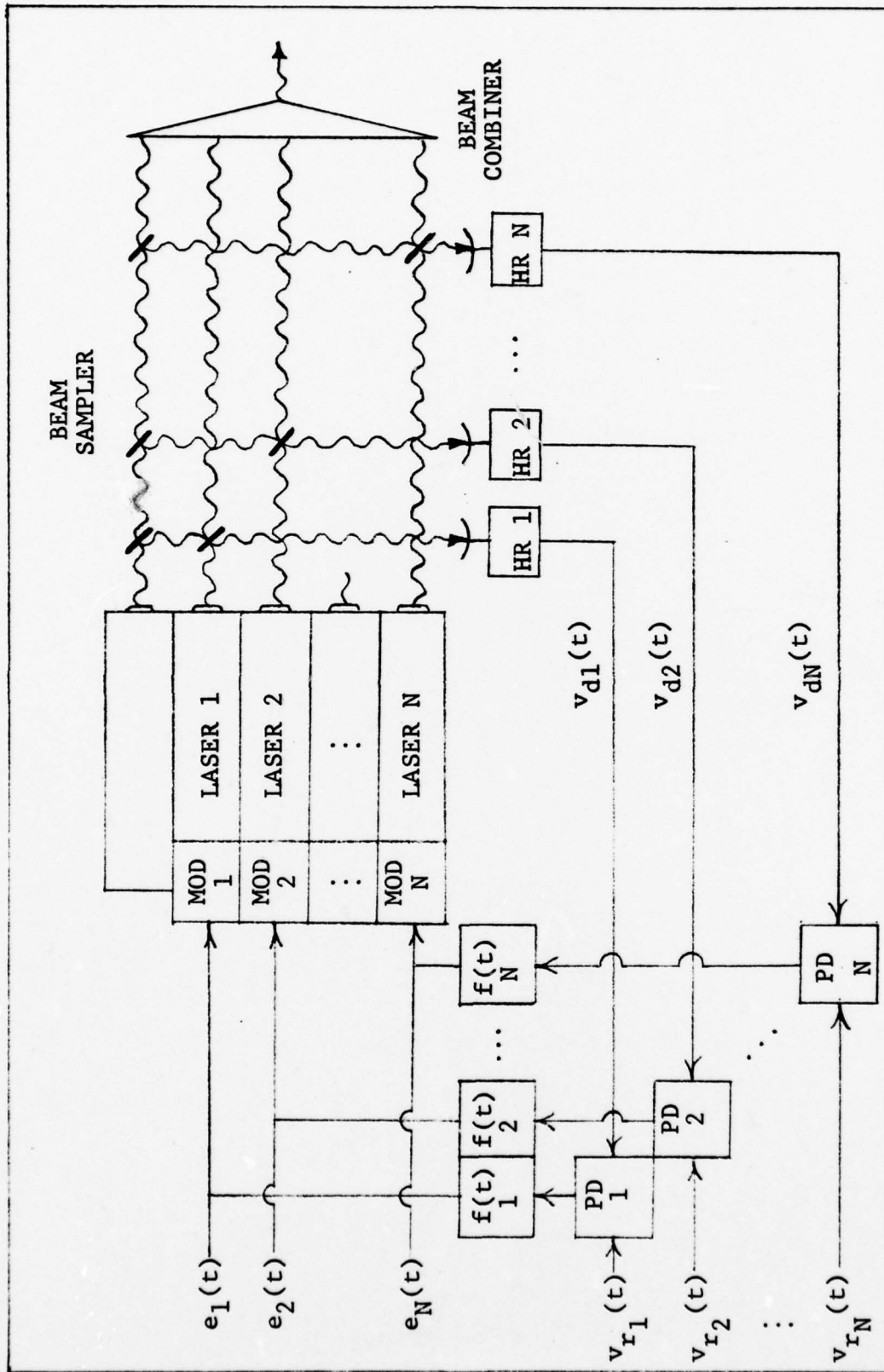


Figure 9. Laser Array Control Loops

independent. The variance between any two different lasers n and m is then

$$\begin{aligned}\sigma_{mn}^2 &= \sigma_{nm}^2 = E[(\phi_m(t) - \phi_n(t))^2] , \quad m \neq n \\ &= E[(\phi_m(t) - \phi_o(t))^2] + E[(\phi_m(t) - \phi_o(t))^2] \quad (129)\end{aligned}$$

and

$$\sigma_{mn}^2 = \sigma_{nm}^2 = \sigma_{on}^2 + \sigma_{om}^2 , \quad m \neq n \quad (130)$$

Since σ_{mn}^2 is a measure of the spread of the differential phase between laser m and n , then if $n = m$, $\phi_m(t) = \phi_n(t)$ and thus

$$\sigma_{mn}^2 = 0 , \quad m = n \quad (131)$$

The array variance is defined in matrix form as

$$\sigma^2 = \begin{bmatrix} \sigma_{00}^2 & \sigma_{01}^2 & \sigma_{02}^2 & \dots & \sigma_{0N}^2 \\ \sigma_{10}^2 & \sigma_{11}^2 & \sigma_{12}^2 & & \sigma_{1N}^2 \\ \sigma_{20}^2 & \sigma_{21}^2 & \sigma_{22}^2 & & \sigma_{2N}^2 \\ \vdots & & & \sigma_{nm}^2 & \vdots \\ \sigma_{N0}^2 & \sigma_{N1}^2 & \sigma_{N2}^2 & \dots & \sigma_{NN}^2 \end{bmatrix} \quad (132)$$

For the single reference array, the array variance σ_A^2 is

$$\sigma_A^2 = \begin{bmatrix} 0 & \sigma_{01}^2 & \sigma_{02}^2 & \sigma_{03}^2 & \dots & \sigma_{0N}^2 \\ \cdot & 0 & (\sigma_{01}^2 + \sigma_{02}^2) & (\sigma_{01}^2 + \sigma_{03}^2) & & (\sigma_{01}^2 + \sigma_{0N}^2) \\ \cdot & & 0 & (\sigma_{02}^2 + \sigma_{03}^2) & & (\sigma_{02}^2 + \sigma_{0N}^2) \\ & & & 0 & & \cdot \\ & & & & & \cdot \\ & & & & \dots & 0 \end{bmatrix} \quad (133)$$

If all the lasers, except perhaps the reference laser, are identical and all n loops have the same performance (e.g., same W_H) then

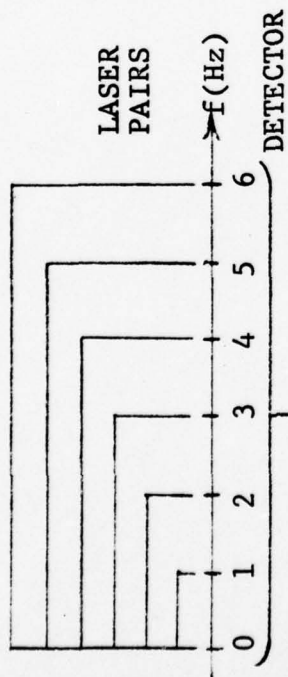
$$\sigma_{0n}^2 = \sigma_{01}^2, \quad 1 \leq n \leq N \quad (134)$$

and the array variance reduces to

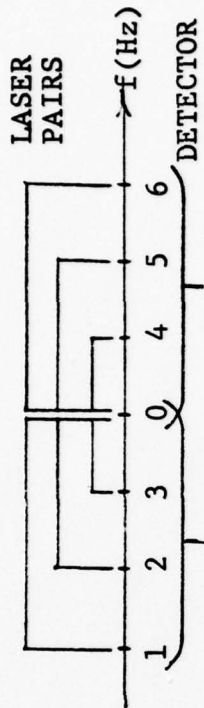
$$\sigma_A^2 = \begin{bmatrix} 0 & \sigma_{01}^2 & \sigma_{01}^2 & \sigma_{01}^2 & \dots & \sigma_{01}^2 \\ \cdot & 0 & 2\sigma_{01}^2 & 2\sigma_{01}^2 & & 2\sigma_{01}^2 \\ \cdot & & 0 & 2\sigma_{01}^2 & & \sigma_{01}^2 \\ & & & 0 & & \cdot \\ & & & & & \cdot \\ & & & & \dots & 0 \end{bmatrix} \quad (135)$$

A simplification possible with this type of array is to combine all the heterodyne receivers into one detector followed by a parallel array of bandpass filters. The reference laser must be placed where no two differential frequencies are the same, probably at the lower or higher frequency end as shown in Figure 10a. If all the assumptions for a heterodyne receiver still hold for each laser pair (e.g., $A_0 \gg A_1, A_2, \dots, A_N$) then each BPF will continue to pass the same signal as before (see Appendix A, Figure A-3). The main advantage of this multiple heterodyne receiver is that it requires $N-1$ less detectors. It is also likely that this will simplify the beam sampling optics since now the reference laser beam is required at only one detector, not N .

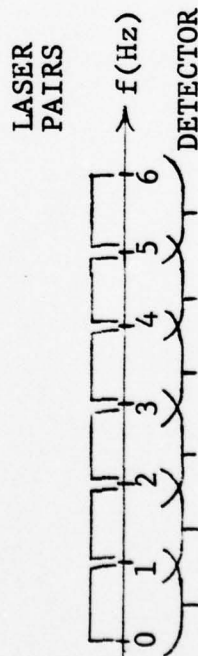
There are some disadvantages however. Where as before each detector needed an active bandwidth (frequency range over which the detector will respond) only wide enough to cover the frequency difference between two lasers, now the detector must be able to respond to the entire frequency range of all laser outputs. Another disadvantage is that no two BPFs can pass the same frequencies. If they could, then a differential phase of one laser pair which drifted or was changed too far would feedback its signal through the wrong loop to the wrong laser modulator. This requirement obviously puts a limit on the flexibility of the system. That is, the differential phase of each laser pair is restricted to a specific range of frequencies and can never crossover into another laser-pair zone (without changing the BPF array).



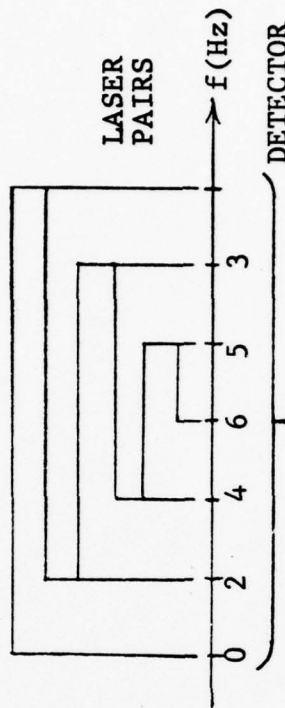
(a) Single Reference Array--
One Detector



(b) Single Reference Array--
Two Detectors



(c) Sequential Array--
N Detectors



(d) Sequential Array--
One Detector

Figure 10. Array Design Tradeoffs in the Frequency Domain (N=6)

A good compromise to restore some flexibility and reduced required detector active bandwidth might be to use two or three detectors and place the reference laser at some central frequency as shown in Figure 10b.

Sequential Array

A sequential array is constructed of $N + 1$ lasers each paired against the next in sequence, "0" with "1", "1" with "2", "2" with "3", etc., as shown in Figure 10c, making a total of N control loops. The only difference between this array and the single reference is in the beam sampling optics represented in Figure 11. The rest of the array is the same as in Figure 9.

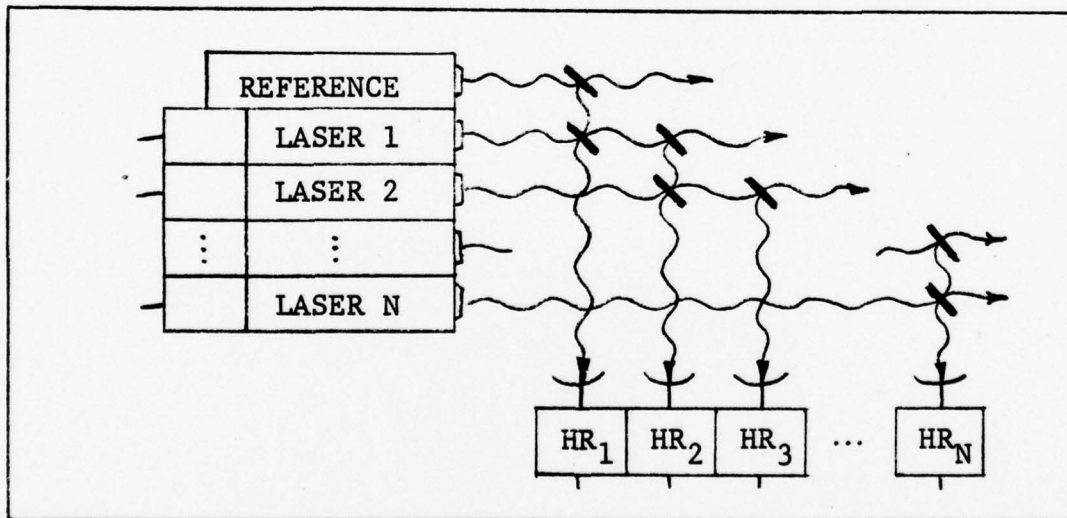


Figure 11. Representation of Beam Sampling Optics for a Sequential Array

Again, the loop reference signals are assumed to be in phase with each other.

Assuming again that the individual loops are uncoupled, the variance of the laser differential phase error for each pair is still given by Eq (77), but the modulated laser of one pair is the reference laser of the next. Thus a change in differential phase anywhere will "ripple" down the remaining laser pairs. If the noise and instabilities of all N lasers are statistically independent then the variance between any two lasers is

$$\begin{aligned} \sigma_{mm}^2 = \sigma_{nn}^2 = & \sigma_{n(n+1)}^2 + \sigma_{(n+1)(n+2)}^2 + \sigma_{(n+2)(n+3)}^2 + \dots \\ & \dots + \sigma_{(m-2)(m-1)}^2 + \sigma_{(m-1)m}^2, \quad n < m \end{aligned} \quad (136)$$

If all N+1 lasers are identical, then

$$\sigma_{n(n+1)}^2 = \sigma_{01}^2, \quad 0 \leq n \leq N-1 \quad (137)$$

and the laser differential phase variance matrix σ_B^2 of the sequential array is

$$\sigma_B^2 = \begin{bmatrix} 0 & \sigma_{01}^2 & 2\sigma_{01}^2 & 3\sigma_{01}^2 & \dots & N\sigma_{01}^2 \\ \cdot & 0 & \sigma_{01}^2 & 2\sigma_{01}^2 & & (N-1)\sigma_{01}^2 \\ \cdot & & 0 & \sigma_{01}^2 & & \cdot \\ & & & 0 & & \cdot \\ & & & & & \cdot \\ & & & & & 0 \end{bmatrix} \quad (138)$$

The further apart in the sequence two lasers are, the proportionally more is the variance between them. This obviously is not as good as the single reference array performance (Eq (135)).

If the lasers are separated by a constant frequency Δf , then the differential frequency for each laser pair is the same. In this case a single detector cannot be used, as in the single reference array, because each BPF must pass the same differential frequency. However, since all loops have the same differential frequency Δf there is no way to distinguish the differential frequency of a given pair. A possible method to circumvent this problem is not to pair the lasers sequentially in frequency. This approach is depicted in Figure 10d. With this configuration the differential frequency for every laser pair is different and can be distinguished by the BPF array. Again, however, each differential frequency is restricted to its own bandpass (determined by the BPF) outside of which it will modulate the wrong laser.

A possibly major disadvantage of the sequential array is that if one laser malfunctions, it will separate into two independent, smaller arrays destroying the device output. A laser malfunction in the single reference array will result in only one beam missing from the device output.

Laser Array Design Considerations

There are several important factors to be considered in the design of any array. Some of these points will be

mentioned here but they are by no means a comprehensive list. It may be helpful to refer to Figure 9 during the discussion.

Loop Reference Control. Early in this discussion it was assumed that the loop reference signals were in phase. Indeed this must be true since the separate laser phase differentials cannot be coherent if the standards to which they are locked are not.

The simplest way to guarantee phase coherence between reference signals is to let them all be the output of a single VCO. This of course places the restriction that all laser differential phases must be the same, that of the VCO.

It is increasingly more difficult to control the differential frequency and phase of each pair separately. This would require phase locking the reference VCOs, or adding a control signal internal to the loop (see Table III). Each of these procedures, however, would add to device complexity.

Single Versus Separate Detectors. The advantage of using a single detector is that it reduces the number of detectors required and thus simplifies the beam sampling optics. However, the disadvantages must be carefully considered.

The active bandwidth of the single detector must range over all laser outputs not just two. This could especially be a problem if the detector response is not uniform (constant for all frequencies).

Also since all differential frequencies are coming from the same detector, the BPFs for the separate PLLs cannot overlap. Thus each laser pair is restricted to a band of frequencies determined by the BPF array. Additionally, limiting the size of the BPFs also limits the bandwidth of the closed-loop transfer function, W_H . This could have a severe effect on differential phase error variance performance and on the dynamic performance.

Separate detectors, although more are required and beam sampling optics may be more complex, have no such restrictions on BPF bandwidth, B_{0n} , and thus on differential frequency operation range. Indeed the BPF may be a high pass filter instead, and cover virtually all frequencies. Also detectors with narrower active bandwidths can be utilized (this will restrict the differential frequency operating range, but not the noise performance).

Stability of the Reference Laser. The phase locked by the basic two-laser control loop is the differential phase between the two lasers, not their absolute phases. The laser pair absolute phase is free to drift throughout the laser bandwidth. This is also true for the array; it is the relative phase among the lasers that is locked, not their absolute phases. If, as is likely, the array utilizes frequencies from as much of the laser gain linewidth as possible, it is entirely possible that the lasers operating near the edge may be forced out of the gain linewidth by a

drifting reference laser. For those lasers, the power out would then drop significantly below the others (or even worse cease to lase) thus having a deleterious effect on the array output field and phase variance. If the power dropped enough, that particular pair would drop out of lock completely.

Thus the absolute frequency stability of the reference laser is of paramount importance. There are many stabilization techniques, but these will not be discussed here (Ref 10:1015-1026). The key design requirement, however, is that the reference laser must have its own characteristics and controls. It is therefore likely that the reference laser should be separate from the array lasers and perhaps not even used in the ultimate array output.

Initial Acquisition. The heterodyne receiver output phase $\phi_d(t)$ is the difference in phase between the two input lasers (Eq (A-12)). However, there is no distinction between which laser has the higher frequency. If the control loop is configured to shift f_1 to a higher frequency when a positive error voltage is applied and if f_0 is initially greater than f_1 , then the loop will drive f_1 up to f_0 where the loop will lock. But if f_0 is initially lower, the loop will still drive f_1 higher and it will never lock. Therefore, if the initial acquisition is to be assured, the reference laser must have a known frequency relative to each of the modulated lasers at system turn-on. This is another good argument for

stabilizing the absolute frequency of the reference laser. If the reference laser were stabilized at one extreme of the modulated lasers operating range even if a laser pair momentarily broke lock, it would automatically be in a position to relock. The control voltage could also be used to "sweep" the modulated frequency to attain lock.

Beam Control. The optics of the laser array must fulfill two functions. First, the beams must be coherently combined and directed towards the desired target. And second, each field must be "sampled" for use in the control loops. For the laser array fields to combine with the desired effect in the far field, several attributes of the fields must be regulated precisely.

Alignment of the sampled beams into the detector is critical since heterodyne detection requires accurately parallel and overlapping incident fields. A difference in angle between the two fields on the order of $\lambda/\text{diameter}$ of detector will result in degraded output (Ref 11:186).

Another difficult problem regards the relative optical path lengths of the beams in the beam combining and beam sampling optics. The control loop for each laser pair locks the laser differential phase of the sampled beam, not the actual output beam, to the reference phase. So while the sampled beams may be perfectly locked by the control array, the actual beams directed towards the target may not be coherent in the desired manner. To avoid this problem, for

each laser pair, the optical distance between the beam sampling points of each beam must precisely equal the optical distance between each sampling point and the beam array output combination point (or be an integer multiple of the wavelength). The optical precision required could be a major consideration in the construction of any array.

These are only some of the array design considerations. Others are mentioned in the suggestions for further study following the summary.

IV. Conclusion

Summary

This paper presented design considerations and fundamental performance limitations of phase locked feedback loops which were used to coherently combine the outputs of an array of single mode, but electronically phase modulated, lasers. The control problem was first investigated in a "two-laser" control loop designed to lock the differential phase between the two lasers to a specified reference phase. An optical heterodyne receiver configuration was used to measure the differential phase between the laser pair. An error voltage proportional to the error between the desired, reference phase and the measured differential phase was filtered and used to frequency modulate one of the lasers in an attempt to null the error. An integro-differential equation, valid for the linearized operating region of the loop was derived in terms of reference phase control, the heterodyne measurement noise, and the various laser phase instabilities. The solution of the equation resulted in the following expression for the laser differential phase error variance in terms of the closed-loop equivalent noise bandwidth of the system, W_H :

$$\sigma_{01}^2 = \hat{C}_1 W_H + \frac{\hat{C}_2}{W_H} + \frac{\hat{C}_3}{W_H^2} \quad (77)$$

The first term was due to heterodyne measurement noise where \hat{C}_1 was proportional to the energy of a detected photon. The second was due to the quantum limited noise of the laser where \hat{C}_2 was proportional to the quantum limited laser field linewidth. The third term was due to external noise on the laser where \hat{C}_3 was proportional to the linewidth of the field (less that due to quantum noise). The conflicting effects of W_H on each term suggested optimization of W_H . Additionally, the relationship between the loop filter and W_H and other system performance parameters such as loop acquisition time, frequency pull-in range and steady state error was examined. A design example was presented to illustrate the effects of various laser, detector and desired phase control parameters on the overall performance of the loop. It was found that the loop performed very well for the specific example presented with a standard phase deviation between the two lasers of less than .1 radian and a lock-up time of no more than 1 μ sec.

The basic pairwise control model was then used to develop control configurations for laser arrays. Two configurations were reviewed: (1) all lasers locked pairwise to the same reference laser and (2) each laser locked pairwise in sequence across the array. Finally, resulting implications of system complexity and potential sources of phase errors across the array were discussed.

Suggestions for Further Study

Several of the assumptions made in this paper may not always hold. For instance, it was assumed in deriving the differential phase variance that the loop reference was relatively stable (Eq (45)). Although treated briefly (Eqs (94) through (96)) a more complete study is in order.

It was also implicit in the discussion but never really stated that lasers operate in one mode, on one transition line only. Active mode competition will have an especially harmful effect on the far field but could also affect the loop control. Discrete jumps in frequency due to vibration/rotational level competition would increase the phase variance. Both these effects are unfortunately enhanced by the mirror movement which may be used to modulate the frequency.

Another assumption was that the lasers in an array were all statistically independent. This may not be true if all the lasers are in the same structure. The external portion of phase noise in this case would be mostly common to all the lasers.

In the same vein, it was assumed that the external noise had a Gaussian density (Appendix B). If it does not, the resulting field phase spectrum becomes very difficult to determine, but may be important if a particular external noise source is persistent (e.g., aircraft vibrations if the device is to be mounted on an aircraft).

Also the field amplitude has instabilities that were neglected (Eq (B-4)). It will have an effect on the far field waveform.

The closed-loop transfer function was modeled as an ideal low-pass filter (Eq (64)). A more accurate description could be found which would include the effects of other loop components (such as heterodyne receiver band pass filter, line impedances, modulator crystal capacitances and loop filter).

Several assumed linearities are especially worth investigating. The laser output power for instance is dependent on where along the gain medium bandwidth the laser is operating. Also the detector may not have a uniform response over its entire active range. Further, the modulator crystal may not respond linearly to large requests for changes in frequency. All of these must be considered in the final evaluation of performance.

The most versatile loop filter, the third order (Table III), presents a mathematically intractable problem. A computer simulation of such a system would help predict loop performance much better than the rough estimates using second order results (Table IV).

The effect on the array output of a single laser ceasing to lase was only briefly mentioned. A more thorough study of possible array configurations and their inherent reliability and sensitivity to equipment malfunctions could be

worthwhile especially if the system is to be used in a hostile environment.

Specific attention should be given to the use of the CO₂ waveguide laser referred to in the example. It combines a relatively wide useable gain bandwidth with single frequency operation (Ref 9:1-33).

There has been one successful attempt to control the phase of a number of CO₂ waveguide lasers (N = 4) and coherently sum their outputs (Ref 12:263-4). Construction of larger arrays with more flexible modulation capabilities could now be considered.

Bibliography

1. Yariv, Ammon. Quantum Electronics. (2nd edition). New York: John Wiley and Sons, Inc., 1975.
2. Viterbi, A. J. Principles of Coherent Communication. New York: McGraw-Hill Book Company, 1966.
3. Yariv, Ammon and W. M. Caton. "Frequency, Intensity, and Field Fluctuations in Laser Oscillators," IEEE Journal of Quantum Electronics. QE-10:509-515. (June 1974).
4. Garner, F. M. Phaselock Techniques. New York: John Wiley and Sons, Inc., 1966.
5. Lindsey, W. C. Synchronization Systems in Communication and Control. Englewood Cliffs, New Jersey: Prentice Hall, Inc., 1972.
6. Siegman, A. E., et al. "Preliminary Measurements of Laser Short-Term Frequency Fluctuations," IEEE Journal of Quantum Electronics. QE-3:180-189 (May 1967).
7. Spilker, J. J. Digital Communications by Satellite. Englewood Cliffs, New Jersey: Prentice Hall, Inc., 1977.
8. Hafnew, E. "The Effects of Noise in Oscillators," Proceedings of the IEEE, 54:179-198 (February 1966).
9. Degnan, J. J. "The Waveguide Lasers: A Review," Applied Physics, 11:1-33 (1976).
10. Birnbaum, G. "Frequency Stabilization of Gas Lasers," Proceedings of the IEEE, 55:1015-1026 (June 1967).
11. Pratt, W. K. Laser Communication Systems. New York: John Wiley and Sons, Inc., 1969.
12. Hayes, C. L. and L. M. Laughman. "Generation of Coherent Optical Pulses," Applied Optics, 16:263-264 (February 1977).
13. Hoversten, E. V. "Optical Communication Theory." in Laser Handbook, edited by F. T. Arecchi and E. O. Schultz-Dubois. Amsterdam: North Holland Publishing Co., 1972.

14. Freed, C. "Design and Short-Term Stability of Single-Frequency CO₂ Lasers," IEEE Journal of Quantum Electronics, QE-4:404-408 (June 1968).
15. Siegman, A. E. and R. Arrathoon. "Observation of Quantum Phase Noise in a Laser Oscillator," Physical Review Letters, 20:901-902 (April 22, 1968).
16. Manes, K. R. and Siegman, A. E. "Observation of Quantum Phase Fluctuations in Infrared Gas Lasers," Physical Review A, 4:373-386 (July 1971).
17. Hinkley, E. D. and C. Freed. "Direct Observation of the Lorentzian Line Shape as Limited by Quantum Phase Noise in a Laser Above Threshold," Physical Review Letters, 23:277-280 (August 11, 1969).
18. Jaseja, T. S., et al. "Frequency Stability of HeNe Masers and Measurements of Length," Physical Review Letters, 10:165-167 (March 1, 1963).
19. Picinbono, B. "Statistical Properties of Randomly Modulated Laser Beams," Physical Review A, 4:2398-2407 (December 1971).
20. Cutler, L. S. and C. L. Searle. "Some Aspects of the Theory and Measurement of Frequency Fluctuations in Frequency Standards," Proceedings of the IEEE, 54:136-154 (February 1966).
21. Papoulis, A. Probability, Random Variables, and Stochastic Processes. New York: McGraw-Hill Book Company, 1965.
22. Dudley, W. W. CO₂ Lasers: Effects and Applications. New York: Academic Press, Inc., 1976.
23. Nye, J. F. Physical Properties of Crystals. London: Oxford University Press, 1957.
24. Ziemer, W. H. Principles of Communications: Systems Modulation and Noise. Boston: Houghton Mifflin, Inc., 1976.

Appendix A

Heterodyne Detection

Heterodyne detection is a measurement technique used to determine the phase of a field relative to a reference field while simultaneously suppressing the effects of thermal and dark current noise present in optical detectors. The first and second moment characteristics of the heterodyne receiver output are presented in this appendix.

The basic heterodyne receiver (HR), depicted in Figure A-1 consists of mixing (adding) two fields together onto the same detector to produce a signal with a phase equal to the differential phase of the fields ("beat frequency").

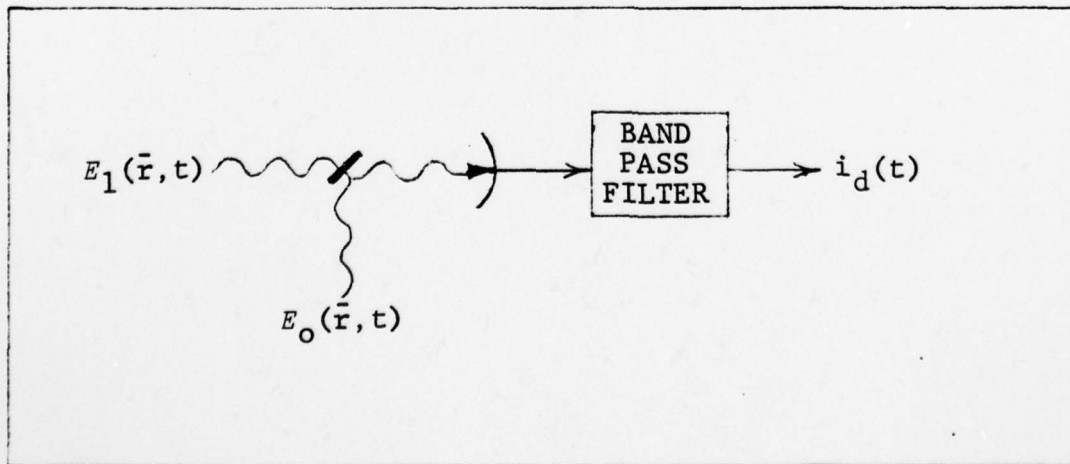


Figure A-1. Basic Heterodyne Receiver Configuration

This signal is then passed through a bandpass filter (BPF) which suppresses the noise relative to the signal. If the phase of one field, $E_o(\bar{r}, t)$ called the local oscillator, is known, then the phase of the other field can be readily determined from the detector output.

The results stated herein are conditional on the following assumptions:

(1) The fields impinging on the detector are collinear, planar, of constant magnitude and normally incident. They can therefore be expressed as

$$E_o(\bar{r}, t) = A_o \cos \phi_o(t) = A_o \operatorname{Re} \left[e^{j\phi_o(t)} \right] \quad (\text{A-1})$$

and

$$E_1(\bar{r}, t) = A_1 \cos \phi_1(t) = A_1 \operatorname{Re} \left[e^{j\phi_1(t)} \right] \quad (\text{A-2})$$

In this paper the $\operatorname{Re}[\]$ will be understood when using the complex envelope notation. Thus the fields will be written as

$$E_o(\bar{r}, t) = A_o e^{j\phi_o(t)} \quad (\text{A-3})$$

and

$$E_1(\bar{r}, t) = A_1 e^{j\phi_1(t)} \quad (\text{A-4})$$

The phases are

$$\phi_o(t) = 2\pi f_{oq} t + \phi_o + \theta_o(t) \quad (\text{A-5})$$

and

$$\phi_1(t) = 2\pi f_{1q}t + \phi_1 + \theta_1(t) \quad (\text{A-6})$$

where f_{oq} and f_{1q} are the respective quiescent frequencies and $\theta_o(t)$ and $\theta_1(t)$ are phase modulation terms which include both control and random phase fluctuations.

(2) For power or energy calculations only,

$$f_o = f_{oq} \approx f_{1q} \quad (\text{A-7})$$

(3) The combined beam is incident on area A_d of the detector, called the active area.

(4) The fields, traveling in free space, have units of volts/m/ $\sqrt{\text{ohm}}$ and without loss of generality,

$$A_o \gg A_1 \quad (\text{A-8})$$

(The reverse, $A_1 \gg A_o$, could also be true but would be included in the following results with a simple change in subscripts.)

(5) There is negligible excess noise. (An "excess noise" term arises strictly from the random portion of the fields (Ref 11:16).)

(6) The BPF is ideal with impulse response $b(t)$, transfer function $|B(j2\pi f)|^2$, magnitude $1/C_{01}^2$, spectral width B_{01} Hz, and centered on frequency

$$f_d = f_{1q} - f_{oq} \quad (\text{A-9})$$

AD-A052 915

AIR FORCE INST OF TECH WRIGHT-PATTERSON AFB OHIO SCH--ETC F/G 20/5
PHASE-LOCK CONTROL CONSIDERATIONS FOR MULTIPLE, COHERENTLY COMB--ETC(U)
DEC 77 J B ARMOR

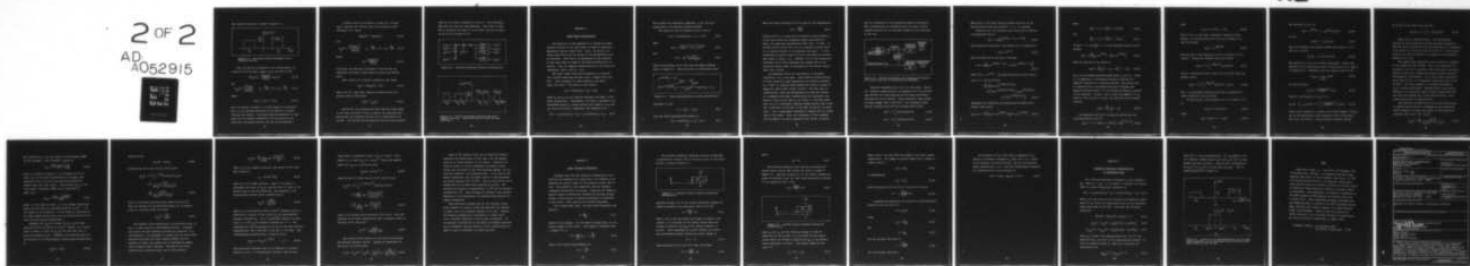
UNCLASSIFIED

AFIT/6E0/EE/77-2

NL

2 OF 2

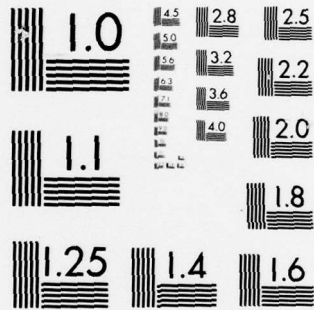
AD
A052915



END
DATE
FILMED

5-78

DDC



MICROCOPY RESOLUTION TEST CHART
NATIONAL BUREAU OF STANDARDS-1963-A

The transform function is shown in Figure A-2.

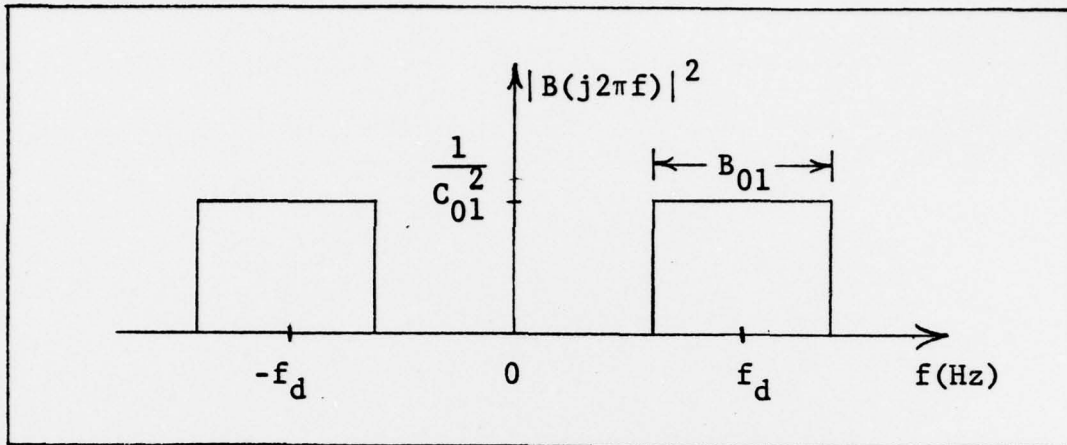


Figure A-2. Heterodyne Receiver Bandpass Filter Transfer Function

With the previous assumptions, the second moment statistics of the HR output current $i_d(t)$ are (Ref 11:187)

$$E[L_d(t)] = \frac{q\eta A_d A_o A_1}{hf_o C_{01}} \cos\phi_d(t) \quad (\text{A-10})$$

and

$$S_{i_d}(f) = \frac{q^2 \eta A_d A_o^2}{2hf_o C_{01}} \quad , \quad f_d - \frac{B_{01}}{2} \leq |f| \leq f_d + \frac{B_{01}}{2} \quad (\text{A-11})$$

where

$$\phi_d(t) = \phi_1(t) - \phi_o(t) \quad (\text{A-12})$$

and h is Planck's constant, q is the charge of an electron and η is the quantum efficiency of the detector in photoelectrons per photon. (All power spectral densities in this paper are the Fourier transform of the covariance of the particular stationary process, not the autocorrelation.)

If these results are desired in terms of a voltage, $v_d(t)$, multiply the current $i_d(t)$ by an effective load resistance R to obtain

$$E[v_d(t)] = V_d \cos \phi_d(t) \quad (A-13)$$

and

$$S_{v_d}(f) = \frac{q^2 \eta A_d A_o^2 R^2}{2 h f_o C_{o1}^2}, \quad f_d - \frac{B_{o1}}{2} \leq |f| \leq f_d + \frac{B_{o1}}{2} \quad (A-14)$$

where

$$V_d = \frac{q \eta A_d A_o A_1 R}{h f_o C_{o1}} \quad (A-15)$$

R includes the effective resistance of the HR plus any additional resistance (load) added to obtain the desired $v_d(t)$.

These results are typically modeled as the signal

$$v_d(t) = E[v_d(t)] + n(t) \quad (A-16)$$

where $n(t)$ is a zero mean, Gaussian random process with spectrum (Ref 13:1820-1823)

$$S_n(f) = S_{v_d}(f) \quad (A-17)$$

The HR will also operate with more than one field added to the local oscillator field as long as the resultant beat frequencies are different and each can be separated by its own BPF. The multiple HR configuration and BPF array transfer

function are shown in Figures A-3 and A-4. The individual BPFs need not have the same magnitude. The output of each BPF is precisely the same as in the basic case and is given by Eqs (A-10) through (A-17).

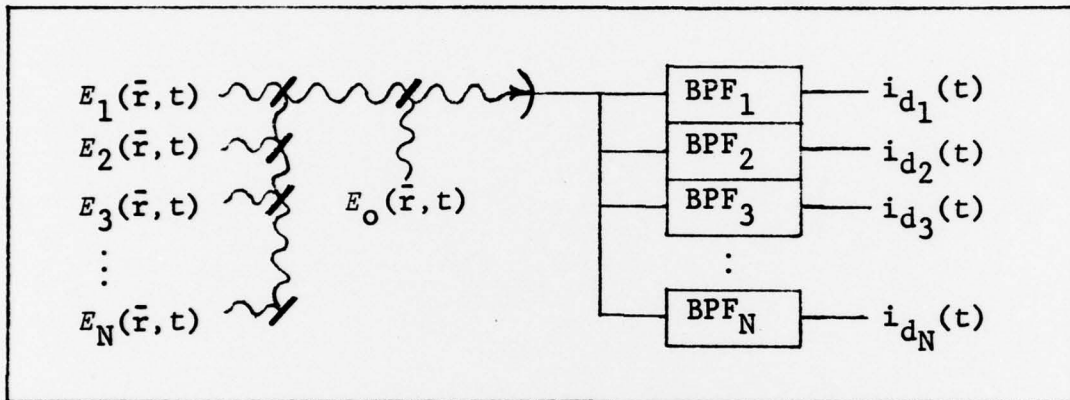


Figure A-3. Multiple Heterodyne Receiver Configuration

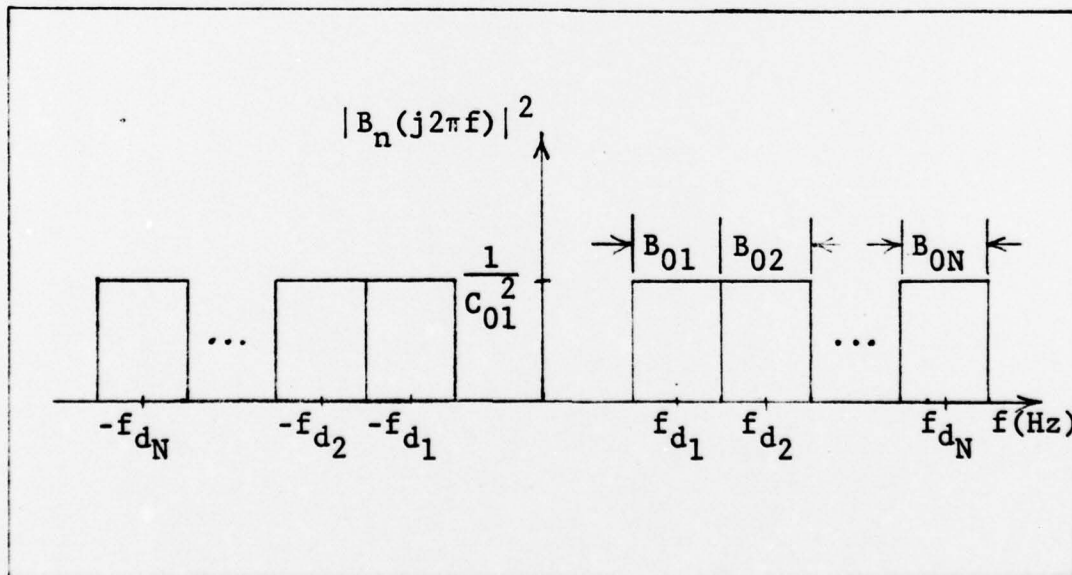


Figure A-4. Multiple Heterodyne Receiver BPF Array Transfer Function. (Each cell need not have the same magnitude.)

Appendix B

Laser Phase Instabilities

The objective of this appendix is to derive the power spectral density of the laser phase in terms of quantities measurable from the laser field. First, the form of the laser output field and the nature of its instabilities will be discussed. From there, an expression for the spectrum of the laser phase in terms of the field spectrum will be derived. Only the temporal characteristics of the field are considered, that is $E(\vec{r}, t) = E(t)$.

The laser output field can be modeled as a sinusoid with constant amplitude and phase plus a random noise term $M(t)$. (This treatment is taken primarily from Yariv (Ref 1:307-318).) The field is thus written:

$$E(t) = A \cos(2\pi f_0 t + \phi_0) + M(t) \quad (\text{B-1})$$

where f_0 and ϕ_0 are the constant frequency and phase of the field respectively. Furthermore, the noise is assumed to be narrowband around f_0 (slowly varying with respect to f_0) and can thus be written in quadrature (see Appendix D) as

$$M(t) = c_n(t) \cos(2\pi f_0 t + \phi_0) + s_n(t) \sin(2\pi f_0 t + \phi_0) \quad (\text{B-2})$$

The in-phase and quadrature components, $c_n(t)$ and $s_n(t)$ respectively, are Gaussian random processes.

The field can also be written in polar form as

$$E(t) = E(t) \cos(2\pi f_0 t + \phi_0 + \gamma(t)) \quad (\text{B-3})$$

where

$$E(t) = \sqrt{s_n^2(t) + (A + c_n(t))^2} \quad (\text{B-4})$$

and

$$\gamma(t) = \tan^{-1} \left(\frac{s_n(t)}{A + c_n(t)} \right) \quad (\text{B-5})$$

These relationships can be seen from the phasor diagram shown in Figure B-1. When the laser is sufficiently above

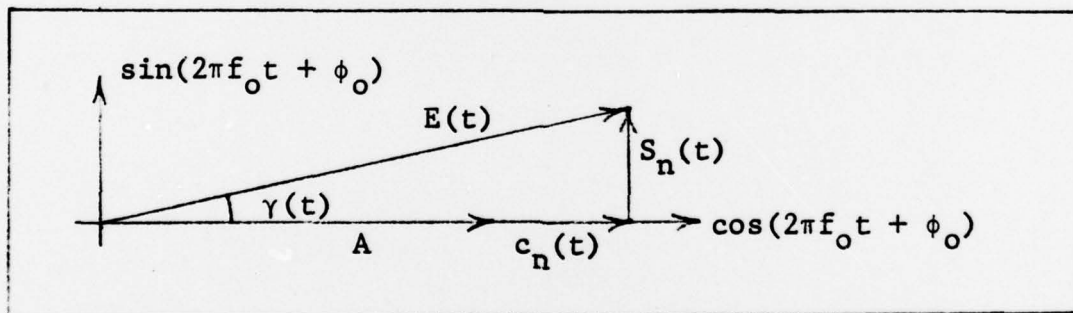


Figure B-1. Phasor Representation of Laser Instabilities

threshold so that

$$A \gg c_n(t), s_n(t) \quad (\text{B-6})$$

then the field representation reduces to

$$E(t) = A \cos(2\pi f_0 t + \phi_0 + \gamma(t)) \quad (\text{B-7})$$

where the phase instability is now given by the approximation

$$\gamma(t) = \frac{s_n(t)}{A} \quad (\text{B-8})$$

From Eq (B-7) it is clear that the spectral characteristics of the laser field are determined almost exclusively by phase, not amplitude instabilities (Ref 6:181; 14:404). It follows from Eq (B-8) that $\gamma(t)$ is a Gaussian process since it is linearly related to the Gaussian term $s_n(t)$. It will arbitrarily be given a mean of zero by including any constant mean terms in $(2\pi f_0 t + \phi_0)$. However, $\gamma(t)$ is not necessarily stationary and in fact represents the random walk of the oscillation phase under the influence of the various noises (Ref 6:181; 14:404).

An assumption about the stationarity of the phase instability $\gamma(t)$ is now made. Laser electric fields because of their inherently high frequencies are typically measured as a "beat" or relative field between two lasers as shown in Figure B-2 (Ref 6:182; 15:901; 16:375). For that type of configuration, where the measurements are made with respect to a standard laser whose instabilities are negligible compared to those of the laser to be tested, it has been shown that $\gamma(t)$ is a stationary, Gaussian random process (Ref 6:180-189; 15:901-902; 16:373-386; 17:277-280; 18:165-167; 19:2398-2407). Such a measurement technique is assumed for all fields used in this paper. Thus, any statements in this appendix (and throughout the text) regarding laser fields or spectra

will be interpreted as the respective measured quantities. This interpretation is consistent with the types of measurements required by the two-laser phaselock loop discussed in the text.

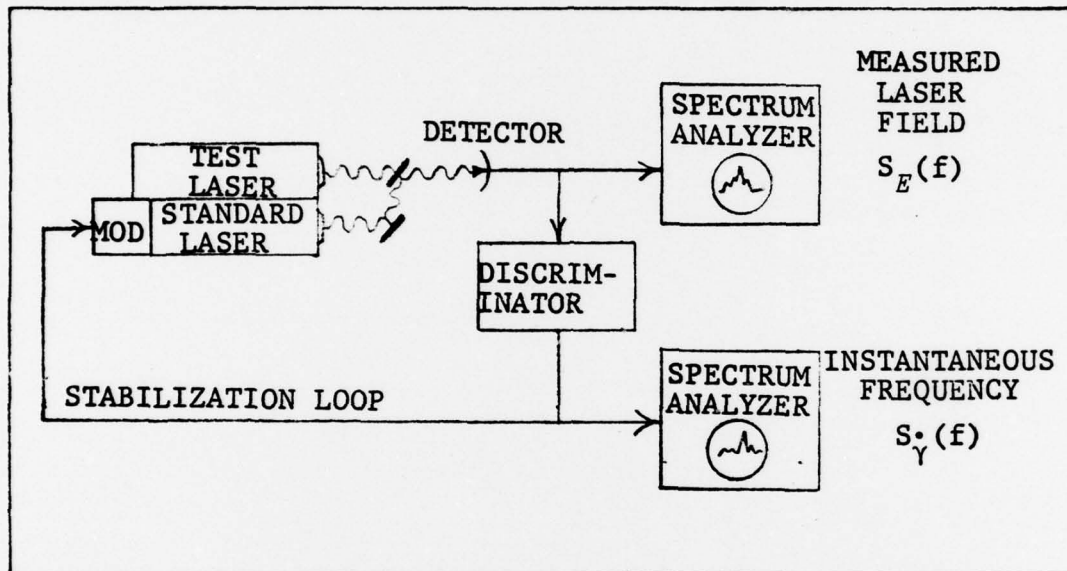


Figure B-2. Typical Arrangement for Measuring the Spectra of a Laser Field and Its Instantaneous Frequency

Using the assumption that $\gamma(t)$ is a zero mean, stationary, Gaussian random process, an expression for the relationship between the field spectrum and the phase instability spectrum can now be derived. (This derivation comes primarily from Siegman (Ref 6:183-184).) The following cosine Fourier transform pair will be utilized (Ref 20:138)

$$S(f) = 2 \int_0^{\infty} R(\tau) \cos(2\pi f\tau) d\tau \quad (B-9)$$

$$R(\tau) = 2 \int_0^{\infty} S(f) \cos(2\pi f\tau) df \quad (B-10)$$

where $S(f)$ is the power spectral density and $R(\tau)$ is the autocorrelation over the interval $\tau = t_2 - t_1$ seconds.

From Eq (B-7), the measured laser field can be written in exponential form as

$$E(t) = A \operatorname{Re} \left[e^{j(2\pi f_0 t + \phi_0 + \gamma(t))} \right] \quad (\text{B-11})$$

For notational convenience, the process $x(t)$ is defined as

$$x(t) = e^{j\gamma(t)} \quad (\text{B-12})$$

Thus the field can be written in the form

$$E(t) = \frac{A}{2} \left[x(t) e^{j(2\pi f_0 t + \phi_0)} + x^*(t) e^{-j(2\pi f_0 t + \phi_0)} \right] \quad (\text{B-13})$$

where $x^*(t) = e^{-j\gamma(t)}$. The autocorrelation of the field is

$$\begin{aligned} R_E(t+\tau, t) &= E \left[E(t+\tau) E^*(t) \right] \\ &= \frac{A^2}{4} E \left[\left(x(t+\tau) e^{j(2\pi f_0(t+\tau) + \phi_0)} \right. \right. \\ &\quad \left. \left. + x^*(t+\tau) e^{-j(2\pi f_0(t+\tau) + \phi_0)} \right) \left(x(t) e^{j(2\pi f_0 t + \phi_0)} \right. \right. \\ &\quad \left. \left. + x^*(t) e^{-j(2\pi f_0 t + \phi_0)} \right) \right] \quad (\text{B-14}) \end{aligned}$$

Expanding this expression and neglecting the double frequency terms yields

$$R_E(t+\tau, t) = \frac{A^2}{4} \left[R_x(t+\tau, t) e^{j2\pi f_0 \tau} + R_x^*(t+\tau, t) e^{-j2\pi f_0 \tau} \right] \quad (\text{B-15})$$

where

$$R_x(t + \tau, t) = E[x(t + \tau)x^*(t)] \quad (B-16)$$

and

$$R_x^*(t + \tau, t) = E[x^*(t + \tau)x(t)] \quad (B-17)$$

If $R_x(t + \tau, t)$ and $R_x^*(t + \tau, t)$ are stationary then Eq (B-15) becomes

$$R_E(\tau) = \frac{A^2}{4} \left[R_x(\tau) e^{j2\pi f_0 \tau} + R_x^*(\tau) e^{-j2\pi f_0 \tau} \right] \quad (B-18)$$

Thus the spectrum of the field is

$$S_E(f) = \frac{A^2}{4} \left[S_x(f - f_0) + S_x^*(-f - f_0) \right] \quad (B-19)$$

This is a two-sided spectrum formed about f_0 and $-f_0$. Since it is impossible to distinguish between a positive or a negative frequency on a spectrum analyzer, this result will be converted into a one-sided spectrum by flipping the negative spectrum about $f = 0$ to overlap the positive portion of the spectrum. If $S_x(f - f_0)$ is real and symmetric on f_0 , which is true if $R_x(\tau)$ is real, the field has the one-sided spectrum

$$S_E(f) = \frac{A^2}{2} S_x(f - f_0) \quad (B-20)$$

An expression for $S_x(f)$ is found by noting that the autocorrelation of $x(t)$ is

$$R_x(t + \tau, t) = E[x(t + \tau)x^*(t)] = E\left[e^{j\Delta\gamma(t, \tau)}\right] \quad (B-21)$$

where

$$\Delta\gamma(t, \tau) = \gamma(t+\tau) - \gamma(t) \quad (\text{B-22})$$

Since $\gamma(t)$ is a zero mean, stationary, Gaussian random process, the autocorrelation of $x(t)$ can be shown to be (Ref 21:159-160)

$$R_x(\tau) = e^{-\frac{1}{2}R_{\Delta\gamma}(0)} \quad (\text{B-23})$$

where $R_{\Delta\gamma}(0)$ is the variance of $\Delta\gamma(t, \tau)$ and $R_x(\tau)$ is stationary. Taking the transform (Eq (B-9)) gives

$$S_x(f) = 2 \int_0^{\infty} e^{-\frac{1}{2}R_{\Delta\gamma}(0)} \cos(2\pi f\tau) d\tau \quad (\text{B-24})$$

Finally, substituting this result into Eq (B-20) gives the general result.

$$S_E(f) = A^2 \int_0^{\infty} e^{-\frac{1}{2}R_{\Delta\gamma}(0)} \cos(2\pi(f - f_0)\tau) d\tau \quad (\text{B-25})$$

Next, a relationship between $R_{\Delta\gamma}(0)$ and the spectrum of phase instability must be found.

To find $R_{\Delta\gamma}(0)$, first express $\Delta\gamma(t, \tau)$ in terms of $\gamma(t)$ as

$$\Delta\gamma(t, \tau) = y(t) * \gamma(t) \quad (\text{B-26})$$

where

$$y(t) = [\delta(t+\tau) - \delta(t)] \quad (\text{B-27})$$

The transform of $y(t)$ is

$$Y(f) = e^{j2\pi f_0 \tau} - 1 = 2je^{j\pi f \tau} \sin(\pi f \tau) \quad (\text{B-28})$$

so that

$$|Y(f)|^2 = 4 \sin^2(\pi f \tau) \quad (\text{B-29})$$

Thus the following relationship between the spectra of $\gamma(t)$ and $\Delta\gamma(t, \tau)$ holds:

$$S_{\Delta\gamma}(f) = 4 \sin^2(\pi f \tau) S_{\gamma}(f) \quad (\text{B-30})$$

The spectrum of $\gamma(t)$ is not readily measurable, however the spectrum of the instantaneous phase instabilities $\dot{\gamma}(t) = \frac{d}{dt}\gamma(t)$ is (Figure B-2). Therefore using the identity (Ref 20:138)

$$S_{\gamma}(f) = \frac{1}{(2\pi f)^2} S_{\dot{\gamma}}(f) \quad (\text{B-31})$$

Eq (B-30) becomes

$$S_{\Delta\gamma}(f) = \left(\frac{\tau \sin(\pi f \tau)}{\pi f \tau} \right)^2 S_{\dot{\gamma}}(f) \quad (\text{B-32})$$

Finally, the variance of $\Delta\gamma_d(t, \tau)$ is

$$R_{\Delta\gamma}(0) = \int_{-\infty}^{\infty} S_{\Delta\gamma}(f) df = 2\tau^2 \int_0^{\infty} \left(\frac{\sin(\pi f \tau)}{\pi f \tau} \right)^2 S_{\dot{\gamma}}(f) df \quad (\text{B-33})$$

(This result differs by a factor of two from Siegman's results due to the definition of the transforms used in this paper, Eqs (B-9) and (B-10).) Using Parseval's general theorem

Eq (B-33) can be recast into the form

$$R_{\Delta\gamma}(0) = 2\tau \int_0^\tau \left(1 - \frac{u}{\tau}\right) R_\gamma(u) du \quad (\text{B-34})$$

These are the desired results. The relationship between the field spectrum $S_E(f)$ and the phase instability spectrum $S_\gamma(f)$ is given by Eq (B-25) where $R_{\Delta\gamma}(0)$ is expressed by Eq (B-33) or (B-34) and $S_\gamma(f)$ by Eq (B-31). These general results will now be related to the specific cases generally observed in a laser.

The random phase instability $\gamma(t)$ of lasers is composed of two components (Ref 15:901). One is an "external" contribution $\gamma_e(t)$ due to acoustic noise, structural vibrations, plasma oscillations, thermal and pressure drifts and other environmental disturbances. (It is also called "technical" noise (Ref 16:373), or "extraneous" modulation (Ref 17:277; 18:165).) The other element is a quantum contribution $\gamma_q(t)$, usually much weaker. Quantum noise is the quantum mechanical or statistical limit of phase fluctuations and thus sets the minimum size of the phase spectrum. This quantum noise will be examined first.

The generally accepted form of the field spectrum due to quantum noise alone for a homogeneous laser operating above threshold at atomic line center is the Lorentzian lineshape (Ref 1:154, 318; 16:374)

$$S_{E_q}(f) = \frac{A^2}{2} \frac{\Delta f_q / 2\pi}{(\Delta f_q / 2)^2 + (f - f_0)^2} \quad (\text{B-35})$$

The variable Δf_q is the full width at half maximum (FWHM) of the lineshape. This linewidth is given by

$$\Delta f_q = \frac{\pi h f_o (\Delta f_{cav})^2}{P} \left(\frac{N_2}{\Delta N} \right) \quad (B-36)$$

where h is Planck's constant, P is the power out of the laser, N_2 is the electron population of the upper laser transition level, and ΔN is the population difference between upper and lower levels. The variable Δf_{cav} is the "cold cavity" bandwidth (FWHM) and is described by (Ref 1:142)

$$\Delta f_{cav} = \frac{c(\alpha_l L - \ln \sqrt{R_1 R_2})}{2\pi L n} \quad (B-37)$$

where c is the speed of light, α_l is an average distributed field loss per pass (not including mirrors) in cm^{-1} , L is the length of the resonator, n is the index of refraction of the laser medium and R_1 and R_2 are the reflectivities of the front and back mirrors respectively.

Assuming that $S_{E_q}(f)$ is known, $S_{\gamma_q}^*(f)$ can be found using Eqs (B-25) and (B-33) or (B-34). However it is easier here to predict a value for $S_{\gamma_q}^*(f)$ and then show that it gives the desired $S_{E_q}(f)$. Therefore the predicted value for the spectrum of the instantaneous quantum phase instabilities is

$$S_{\gamma_q}^*(f) = 2\pi \Delta f_q \quad (B-38)$$

From Eq (B-33)

$$R_{\Delta\gamma}(0) = 2\pi\Delta f_q \tau \quad (\text{B-39})$$

Substituting this value into Eq (B-25) gives

$$\begin{aligned} S_{E_q}(f) &= A^2 \int_0^{\infty} e^{-\pi\Delta f_q \tau} \cos(2\pi(f-f_0)\tau) d\tau \\ &= A^2 \frac{\pi\Delta f_q}{(\pi\Delta f_q)^2 + (2\pi(f-f_0))^2} \\ &= \frac{A^2}{2} \frac{\Delta f_q/2\pi}{(\Delta f_q/2)^2 + (f-f_0)^2} \end{aligned} \quad (\text{B-40})$$

This is the desired field spectrum stated in Eq (B-35).

Thus the spectrum of the phase fluctuation due to quantum noise is, from Eqs (B-38) and (B-31)

$$S_{\gamma_q}(f) = \frac{\Delta f_q}{2\pi f^2} \quad (\text{B-41})$$

The external noise contribution, as previously noted, is due to a wide variety of environmental factors. Although each factor may have different statistical properties (i.e., non-Gaussian), it is reasonable to assume that the laser field spectrum resulting from their combined effects will be Gaussian in shape, and indeed this is confirmed by experimental evidence (Ref 6:180-189). The form of the field spectrum due to external noise only is thus given as

$$S_{E_e}(f) = \frac{A^2}{2} \frac{1}{\sqrt{2\pi\sigma_e^2}} \exp \left[-\frac{(f-f_o)^2}{2\sigma_e^2} \right] \quad (\text{B-42})$$

where σ_e is the standard deviation (rms width) of the curve and is given by

$$\sigma_e = (8 \ln 2)^{-\frac{1}{2}} \Delta f_e \quad (\text{B-43})$$

where Δf_e is the FWHM linewidth. Again it is easier to anticipate the value of $S_{\gamma_e}^*(f)$ and show that it leads to the proper value of the field spectrum. The spectrum of the instantaneous external phase instabilities is

$$S_{\gamma_e}^*(f) = \frac{4\pi\sigma_e^2 f_c}{f_c^2 + f^2} \quad (\text{B-44})$$

where f_c is an arbitrarily small "cutoff" frequency which is effectively a measure of how closely $S_{E_e}(f)$ approximates a Gaussian distribution. If it is perfectly Gaussian in shape then $f_c = 0$ and $S_{\gamma_e}^*(f)$ becomes an impulse at $f = 0$. The approximately $1/f^2$ relationship of Eq (B-44) has been verified experimentally (Ref 6:180-189; 14:901-902; 17:373-386). The corresponding autocorrelation is from Eq (B-10)

$$R_{\gamma_e}^*(\tau) = (2\pi\sigma_e)^2 e^{-2\pi f_c \tau}, \quad \tau \geq 0 \quad (\text{B-45})$$

This expression indicates that f_c is difficult to actually measure in that τ , the observation interval, must be very

large before a measurable decay in $R_{\gamma_e}(\tau)$ occurs. Since ideally f_c is small $R_{\gamma_e}(\tau) \approx (2\pi\sigma_e)^2$. Using this approximation for $R_{\gamma_e}(\tau)$ in Eq (B-34) gives

$$R_{\Delta\gamma}(0) = (2\pi\sigma_e)^2 \tau^2 \quad (\text{B-46})$$

Substituting this value into Eq (B-25) finally gives

$$\begin{aligned} S_{E_e}(f) &= A^2 \int_0^\infty e^{-\frac{1}{2} (2\pi\sigma_e)^2 \tau^2} \cos(2\pi(f-f_0)\tau) d\tau \\ &= A^2 \frac{\sqrt{2\pi}}{4\pi\sigma_e} \exp \left[-\frac{(2\pi(f-f_0))^2}{2(2\pi\sigma_e)^2} \right] \\ &= \frac{A^2}{2} \frac{1}{\sqrt{2\pi\sigma_e^2}} \exp \left[-\frac{(f-f_0)^2}{2\sigma_e^2} \right] \end{aligned} \quad (\text{B-47})$$

which is the desired field spectrum of Eq (B-42). Thus the spectrum of the phase instabilities due to external noise is, from Eqs (B-44) and (B-31)

$$S_{\gamma_e}(f) = \frac{f_c \sigma_e^2}{\pi f^2 (f_c^2 + f^2)} \quad (\text{B-48})$$

The observed field spectrum is the sum of the quantum and external spectrum results. Adding the expressions of Eqs (B-41) and (B-48) gives

$$S_{\gamma}(f) = S_{\gamma_q}(f) + S_{\gamma_e}(f) = \frac{1}{2\pi f^2} \left[\Delta f_q + \frac{2\sigma_e^2 f_c}{(f_c^2 + f^2)} \right] \quad (\text{B-49})$$

Much of the external noise can be removed by careful isolation and construction of the laser, but the quantum noise is of course inherent in all lasers. Typically the external noise so totally overwhelms the quantum contribution that the shape of the field spectrum appears, for all practical purposes, to be Gaussian only. It is only in the higher frequencies that the wider "tails" of the Lorentzian may become apparent (Ref 16:384). This is also obvious from examination of the phase noise spectrum Eq (B-49). The quantum contribution is proportional to $1/f^2$ and the external contribution $1/f^4$. Thus although the external noise clearly dominates at low frequencies, the quantum noise persists to higher frequencies.

This derivation assumed that all the external noises acted together to create a field spectrum that was Gaussian in shape, and this in general appears to be true. However the Gaussian assumption is destroyed if a single noise (e.g., aircraft vibrations or 60 Hz hum) is dominant. If its specific contribution to the field or frequency spectrum can be estimated, then Eq (B-25) or (B-31) respectively can again be used to determine its phase spectrum.

Appendix C

Laser Frequency Modulation

Although there are many methods of modulating or stabilizing the frequency of a laser field, the simplest is by changing the optical length of the resonator cavity (Ref 22: 116). This method is also compatible with the feedback techniques discussed in this paper. Typically the change in optical length is affected by changing the driving voltage across a crystal which is mounted internally or externally to the cavity. Both types will be briefly discussed.

For a single mode laser, the axial mode frequencies are given by

$$f = \frac{mc}{2L_\lambda} \quad (C-1)$$

where m is an integer, c is the speed of light and L_λ is the optical length of the cavity. The change in frequency with a change in L_λ is

$$df = \frac{-mc}{2L_\lambda^2} dL_\lambda = -f \frac{dL_\lambda}{L_\lambda} \quad (C-2)$$

which can be written approximately as

$$\Delta f = - \frac{\Delta L_\lambda}{L_\lambda} f \quad (C-3)$$

The external modulation technique consists of mounting a piezoelectric crystal (PE) on the back of one of the cavity mirrors as shown in Figure C-1.

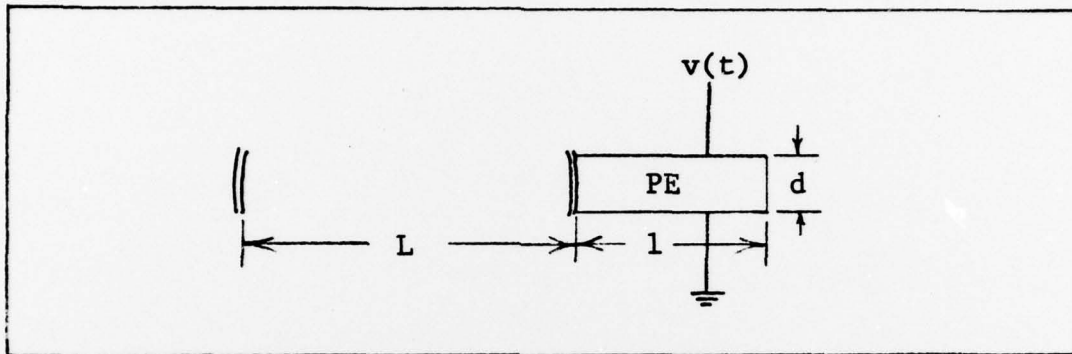


Figure C-1. External Crystal Frequency Modulation Configuration

Applying voltage $v(t)$ to the crystal physically changes its length according to the expression (Ref 23:115-116)

$$\Delta l = \frac{d_{PE} l}{d} v(t) \quad (C-4)$$

where l and Δl are the length and change in length of the crystal, d is the width of the crystal across which the voltage is applied, and d_{PE} is the crystal constant in m/volts. Since expanding the crystal shrinks the cavity, the relationship between crystal and cavity length is

$$\Delta L = - \Delta l \quad (C-5)$$

Substituting Eqs (C-4) and (C-5) into (C-3) gives

$$\Delta f = f \frac{d_{PE} l}{L \lambda d} v(t) \quad (C-6)$$

where

$$L_{\lambda} = nL \quad (C-7)$$

The internal modulation case consists of mounting an electro-optic crystal (EO) inside the cavity as shown in Figure C-2. Applying voltage $v(t)$ to the crystal changes the index of refraction that the laser field encounters according to the expression (Ref 1:347)

$$\Delta n_o = \frac{n_o^3 r_{EO}}{2d} v(t) \quad (C-8)$$

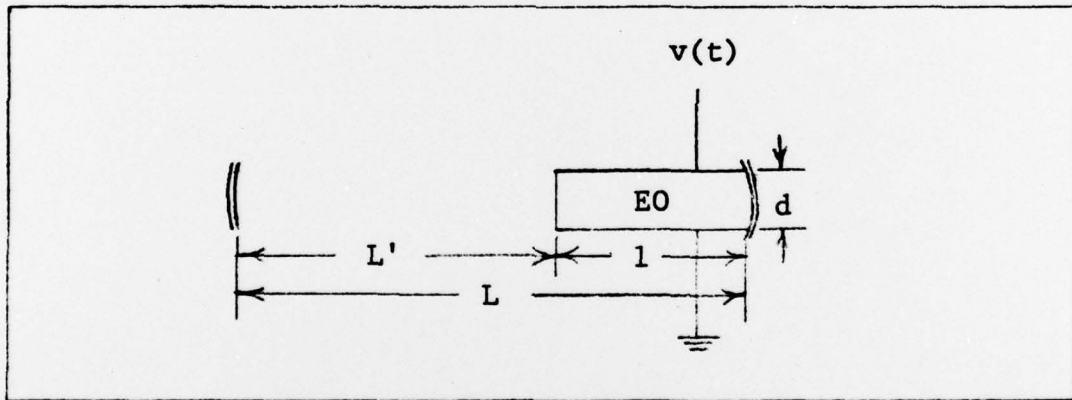


Figure C-2. Internal Crystal Frequency Modulation Configuration

where n_o and Δn_o are the index and change in index of refraction of the crystal, d is the width of the crystal across which the voltage is applied and r_{EO} is the electro-optic coefficient in m/volt. The optical length of the cavity is

$$L_{\lambda} = nL' + n_o l \quad (C-9)$$

where n and L' are the index and length of the laser medium respectively. The change in optical length with a change in crystal index is

$$dL_{\lambda} = ldn_o \quad (C-10)$$

or approximately

$$\Delta L_{\lambda} = l\Delta n_o \quad (C-11)$$

Substituting Eqs (C-8) and (C-11) into Eq (C-3) gives

$$\Delta f = -f \frac{n_o^3 r_{EO}}{2L_{\lambda} d} v(t) \quad (C-12)$$

A generalized expression for either EO or PZT modulation from Eqs (C-6) and (C-12) is

$$\Delta f = K_m v(t) \quad (C-13)$$

where

$$K_m = f \frac{l\epsilon}{L_{\lambda} d} \quad (C-14)$$

and

$$\epsilon = d_{PE} \quad (C-15)$$

for the external (PE case) or

$$\epsilon = \frac{-n_o^3 r_{EO}}{2} \quad (C-16)$$

for the internal (EO case).

The frequency of the laser then is composed of its natural or quiescent frequency f_q (when $v(t) = 0$), a modulated frequency as described above, and any instantaneous phase instabilities, $\gamma(t)$. Thus the instantaneous frequency of a modulated laser can be written as

$$\dot{\phi}(t) = 2\pi(f_q + K_m v(t)) + \dot{\gamma}(t) \quad (C-17)$$

Appendix D

Quadrature Component Representation of Narrowband Noise

For a system operating at frequency f_d with bandwidth B_{01} , where $f_d \gg B_{01}$, it is common to represent the system noise in terms of quadrature components as

$$n(t) = n_c(t)\cos(2\pi f_d t + \phi_d) + n_s(t)\sin(2\pi f_d t + \phi_d) \quad (D-1)$$

where $n_c(t)$ and $n_s(t)$ are the in-phase and quadrature components of the noise $n(t)$ respectively and ϕ_d is an arbitrary phase angle (Ref 24:237-244). They have the following properties

$$E[n(t)] = E[n_c(t)] = E[n_s(t)] = 0 \quad (D-2)$$

$$S_{n_c}(f) = S_{n_s}(f) = L_p[S_n(f-f_d) + S_n(f+f_d)] \quad (D-3)$$

$$S_{n_s n_c}(f) = S_{n_c n_s}(f) = jL_p[S_n(f-f_d) - S_n(f+f_d)] \quad (D-4)$$

where $L_p[]$ means "the lowpass portion of," $E[]$ is the expected value, and $S(f)$ is the power spectral density. If $S_n(f)$ is symmetric about f_d , then $n_c(t)$ and $n_s(t)$ are uncorrelated and

$$R_{n_s n_c}(\tau) = R_{n_c n_s}(\tau) = 0 \quad (D-5)$$

where $R(\tau)$ is the autocorrelation. If, in addition, $n(t)$ is a Gaussian random process $n_c(t)$ and $n_s(t)$ will be independent Gaussian processes. From Eq (D-3) the magnitude of $S_{n_c}(f)$ (or $S_{n_s}(f)$) is twice that of $S_n(f)$. This is shown graphically in Figure D-1.

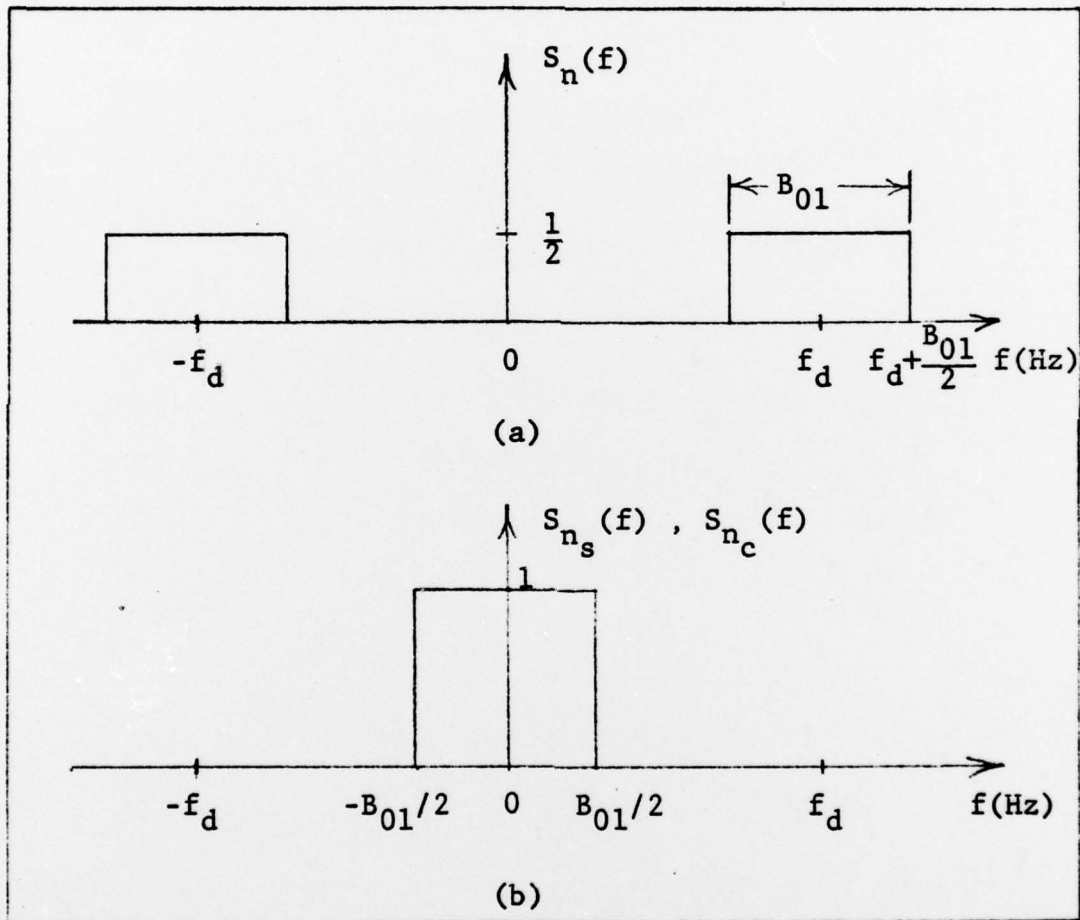


Figure D-1. Spectra of (a) Narrowband Noise and (b) Quadrature Components of the Narrowband Noise with $S_n(f)$ Symmetric about f_d (Ref 22:242)

Vita

James Burton Armor, Jr., was born on 25 September 1950 in Oklahoma City, Oklahoma. He graduated from West Essex Regional High School in North Caldwell, New Jersey, in 1968. He attended Lehigh University in Bethlehem, Pennsylvania, from 1968-1973 where he received a Bachelor of Science degree in Electrical Engineering and a Bachelor of Science degree in Psychology. Upon graduation, he received a commission in the USAF through the ROTC program and entered active duty 1 October 1973. After completing training at Sheppard AFB and Vandenburg AFB, he served in the 381st Strategic Missile Wing, McConnell AFB, Wichita, Kansas, as a Deputy Missile Combat Crew Commander. There he held the position of Senior Instructor until entering the School of Engineering, Air Force Institute of Technology, in August 1976.

Permanent address: 312 Wildberry Road
Pittsburgh, Pennsylvania 15238

UNCLASSIFIED

SECURITY CLASSIFICATION OF THIS PAGE (When Data Entered)

REPORT DOCUMENTATION PAGE		READ INSTRUCTIONS BEFORE COMPLETING FORM
1. REPORT NUMBER AFIT/GEO/EE/77-2 ✓	2. GOVT ACCESSION NO.	3. RECIPIENT'S CATALOG NUMBER
4. TITLE (and Subtitle) PHASE-LOCK CONTROL CONSIDERATIONS FOR MULTIPLE, COHERENTLY COMBINED LASERS		5. TYPE OF REPORT & PERIOD COVERED MS Thesis
7. AUTHOR(s) James B. Armor, Jr. Captain USAF		6. PERFORMING ORG. REPORT NUMBER
9. PERFORMING ORGANIZATION NAME AND ADDRESS Air Force Institute of Technology (AFIT-EN) Wright-Patterson AFB, Ohio 45433		8. CONTRACT OR GRANT NUMBER(s)
11. CONTROLLING OFFICE NAME AND ADDRESS		10. PROGRAM ELEMENT, PROJECT, TASK AREA & WORK UNIT NUMBERS
		12. REPORT DATE December 1977
		13. NUMBER OF PAGES 121
14. MONITORING AGENCY NAME & ADDRESS (if different from Controlling Office) Air Force Avionic Laboratory (AFAL-DHO) Air Force Systems Command Wright-Patterson AFB, Ohio 45433		15. SECURITY CLASS. (of this report) Unclassified
		15a. DECLASSIFICATION/DOWNGRADING SCHEDULE
16. DISTRIBUTION STATEMENT (of this Report) Approved for public release; distribution unlimited		
17. DISTRIBUTION STATEMENT (of the abstract entered in Block 20, if different from Report)		
18. SUPPLEMENTARY NOTES Approved for public release; IAW AFR 190-17 <i>Jerry F. Guess</i> JERRAL F. GUESS, Captain, USAF Director of Information		
19. KEY WORDS (Continue on reverse side if necessary and identify by block number) Phase Control Phase Locked Systems Laser Control Laser Control Systems		
20. ABSTRACT (Continue on reverse side if necessary and identify by block number) This paper presents design considerations and fundamental performance limitations of phase-lock control loops used to coherently combine an array of lasers. A two-laser control loop designed to lock the differential frequency/phase between two lasers to a specified reference is first investigated. An integro-differential equation, valid for the linearized operating region of the loop, is derived in terms of the specified (desired) phase		

next page

UNCLASSIFIED

SECURITY CLASSIFICATION OF THIS PAGE(When Data Entered)

control, the phase measurement (heterodyne) noise, and the laser phase noise (instabilities). Solution of the equation results in an expression for the lasers' phase error variance in terms of the closed-loop noise equivalent bandwidth, the 100 measurement noise, and the lasers' field linewidths. Loop acquisition time, frequency pull-in range, and steady state phase error are also examined. A design example using a CO₂ laser pair is presented and found to have an rms phase deviation of less than .1 rad and a lock-up time of no more than 1 μsec. The basic pairwise model is then used to construct two array configurations: (1) all lasers paired to the same reference laser and (2) each laser locked to the next in sequence. Resulting implications of system complexity and potential phase errors across the array are discussed.

UNCLASSIFIED

SECURITY CLASSIFICATION OF THIS PAGE(When Data Entered)